Chapter 2

DAP Derived Fatty Acid Amide Organogelators as Novel Carrier for Drug Incorporation and pH-Responsive Release

2.1 Introduction

A diverse range of pharmaceutical drugs have been studied for various therapeutic applications over the years. But now they are less preferred because of their low solubility in water.[1] Pharmaceutical industries are facing a major challenge for developing new pharmaceutical products because 40% of the active pharmaceutical ingredients are either moderately soluble or insoluble in aqueous medium.[2] Therefore, pharmaceutical drugs have been subjected to enormous efforts to improve their low water solubility.[3] It is also essential to seek new techniques for fast administration of active values regarding targeted drug delivery methods because of low membrane permeability and bioavailability of pharmacology.

During recent years, self-assembled composites have been investigated as vehicles for delivering molecular cargo to target sites in a sustained manner.[4] However, it has been found that the most productive strategy to accomplish these conditions is to encapsulate the drugs within the gels.[5]

A gel is a three-dimensional cross-linked network structure with an immobilized solution phase that can trap large amounts of solvent, such as water (hydrogel) or organic solvent (organogel).[6] Bigels and emulgels are new classes of gels which are recently reported in the literature.[7] Hydrogen bonds, van der Wall forces, and π-π stacking are the interactions between the gels.[8-10]

As reviewed by Peppas *et al.*, hydrogels have a variety of applications in pharmaceuticals and other fields[11] while organogels have gained the interest of researchers since the late 1990s.[12,13] Organogels are widely studied in areas such as in self-healing materials,[14] fat-free food products,[15] pollutant removal,[16] drug delivery

methods,[17] purification and analysis-related systems.[18] Organogels paved their way towards drug delivery formulations, along with their ease of development and administration. The structural orientation of the LMWGs and the nature of the organic phase are thought to be critical factors in optimizing sustained drug release.[19] The main goal in drug delivery science is to fully control the location, quantity and timing of drug dosing so that the therapeutic effect is maximized and adverse impacts are minimized.[20,21] Organogels on the other hand are insensitive to moisture and are known to penetrate the skin better. Moreover, their organic nature also protects them against microbial contamination thus, their entrapment and gelation processes are straight forward and easy to handle. Long-term use of these materials is safe because they are biocompatible, non immunogenic and biodegradable. So, several drug depot systems have been developed using this gel-developing nature. Organogels, however, offer a number of advantages as a type of drug carrier. But very few studies have been done in evaluating the potential of organogelators in the delivery of drugs.[22]

On the other hand, there is currently a huge interest for drug delivery through skin. Over the past two decades, transdermal and topical drug delivery has increased significantly because of its easy management and accessibility. Nowadays, skin exposure to UV-radiations is the main cause of skin cancer in human beings. For such a cause, organogels can be a doable alternative by delivering anticancer drugs via such vehicles, which has not been tried until date.[23] The delivery of drug molecules through the skin is considered as one of the most essential modes of transmission but it is rather tough when transdermal drug delivery is to be done. Among the numerous strategies studied for improving the delivery of drug molecules through the pores and skin majorly includes the use of penetration enhancers. The fatty acid alcohols and related esters

serve as enhancers for drug permeation for both transdermal and topical drug delivery. Additionally, such type of administration may also assist in avoiding regular effects resulting from oral delivery of nonsteroidal anti-inflammatory drug (NSAIDs) like nausea, gastric irritation, stomach ache, diarrhea and flatulence.

Furthermore, it can also complement to oral remedy for delivering better treatment in situations such as arthritis. One of the most troublesome things for the structural improvement in low atomic weight gelators is the way to stabilize the fashioned gel. In other words, how to avoid the change of state of a metastable gel into crystalline.[24] Moreover raw components like lecithin and other ordinary basis materials are also expensive and inaccessible for vast scope manufacturing. Thus, to overcome these obstacles, amino acid-based fabricated organogelators were used instead of these ordinary raw components.[25,26]

To this end, a unique yet effective gel designed for effective and transdermal utilizations of NSAIDs with expanded enhancer properties has been arranged. Natural liquids having enhancer properties have been picked as gelation solvents for other medication releasing framework. For this design FAE's (Fatty acid isopropyl and ethyl esters) with various chain lengths, ethyl palmitate, ethyl laurate, ethyl myristate, isopropyl myristate, isopropyl laurate and isopropyl palmitate have been picked as biocompatible natural liquids which are broadly utilized in cosmetic and pharmaceutical industries.

Despite of all these advantages, bigels have better properties than single gels,[27] having the advantages of both phases.[28] They are stabilized by trapping of the mobile phases through a three dimensional network of gel by bringing an additional fine dispersion. Bigels are

known to be electrically conductive in nature because of the presence of water pockets in the bigels which permit electrical conduction.[29] For pharmaceutical formulations, bigels have numerous advantages over other semi-solid frameworks that incorporate the synergistic impact of the both gels, ease of development, absence of surfactants related poisonousness and probable delivery of both hydrophilic and lipophilic medications. As no extensive research has been carried out until this point, bigel frameworks may experience some drawbacks like phase partition because of the absence of an emulsifier. In addition, they are not thermo-reversible as they might get weakened at higher temperatures.[30] To be noted that the idea of bigels is somewhat new and very less reports are available in the various areas of applications of bigels specially in the drug delivery. Almeida *et al.* (2008) reported first time the formation of bigels by mixing of oleogels and hydrogel. They assessed bigels based on mechanical properties, stability and moisturising effect.[30] Michele and Varrato *et al.* (2012) reported the self-assembled bigels by encapsulating separate gels in binary colloidal combinations.[31] Again in 2014, the researchers revealed combination dynamics, mechanical properties and structure of colloidal bigels.[32] Ibrahim *et al.* (in 2013) developed different bigel framework by mixing organogels and hydrogels in various proportions. They revealed a comparative study of the hydrogels, organogels and bigels for the transdermal transportation of diltiazem hydrochloride.[33] Bigels have been known to be a great asset as delivery matrices for effective topical applications. It has affinity to transport both hydrophobic and hydrophilic agents,[34] spreadability,[35] moisturizing and cooling effect,[36] washed easily after use,[36] better skin permeability[36] and has greater stability at room temperature.[37] All these properties makes the bigels an attractive choice for cosmetic, aqueous phase and pharmaceutical applications and they have received extensive research in the past decade,

particularly for drug delivery applications.[38,39] But, there is a huge requirement of extensive investigation of the properties and potential uses of the bigels.

In literature, a number of naturally occurring amino acid fatty acid amides have been described as gels capable of delivering drugs.[40-45] Gelators are restricted in their uses in drug delivery systems due to burst release of pharmaceuticals. In order to resolve this issue, Hu and coworkers developed formulation compositions using amino acids as gelators (L-alanine acid, L-serine acid, L-glutamic acid).[46] In previous reports, it was observed that the thermal stabilities and mechanical strength of the gels improved with increased side chain lengths of fatty acids.[47] Nevertheless, this procedure is not very exciting in terms of its large-scale production since natural amino acids are not readily available.

Recently DAP (2,6-diaminopyridine) has received huge attention because of its inimitable symmetric depiction such as their macrocyclic synthetic receptors[48] and hydrogen bonding motifs.[49] Although, self-assembling derivatives of 2,6-diaminopyridine have already been reported in numerous literatures for the formation of nanotubes, nanofibres and nanosheets with applications in biochemistry, medicine and materials science.[50,51] However, the gelating behavior of 2,6-diaminopyridine derived fatty acid amides of varying lengths has not been studied yet. Considering the various applications of organic and bigels, we have focused on the synthesis of a scaffold which could easily self-assemble in different solvents and provide as a substitute to lecithin like gelators, which are expensive and are not suitable for large scale manufacturing. The precise advantage of these derivatives is its simple yet practical synthesis that makes this approach excellent for the fatty acid amide gelators synthesis. In this context, various

analogues of DAP-derived fatty acid amide bi- and organogelators (DMSO is used as a solvent which is biocompatible) were synthesized for drug incorporation and pH responsive release study. Organogel's susceptibility for delivery of NSAID is studied by the use of ibuprofen as a model drug because of the fact that it may interact with the gel not only *via* van der Waal forces, but because of the carboxylic acids moiety, hydrogen bonding could also be retained in the gel. In addition to this, UV-active nature of ibuprofen makes subsequent research less complicated while using UV-spectroscopy techniques. Moreover, the study of drug encapsulation and its release in bigels sustains.

2.2 Experimental

2.2.1 General procedure for the syntheses of DAP derived fatty acid amide gelators

Table 2.1: Synthesis of DAP derived fatty acid amides[a]

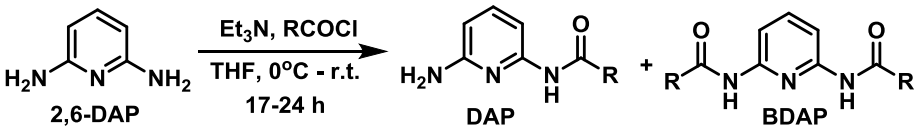

entry	(R)	time (h)	yield (%)[b] DAP	yield (%)[b] BDAP
1	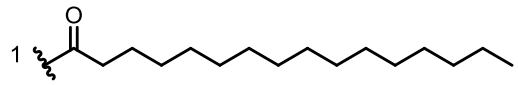	24	**16DAP** (81)	**16BDAP** (8)
2	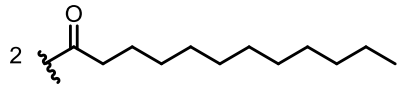	22	**12DAP** (75)	**12BDAP** (10)
3	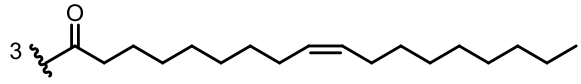	17	**18UDAP** (79)	**18UBDAP** (trace)
4	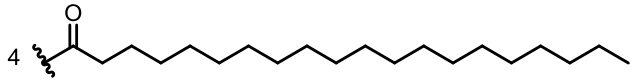	20	**20DAP** (87)	–
5	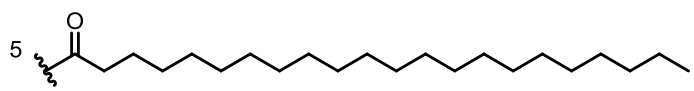	22	**22DAP** (90)	–

[a]Reaction condition: 2,6-DAP (1 mmol), anhyd. Et_3N (2 mmol), RCOCl (1 mmol), anhyd. THF (10 mL); [b]Isolated yield of purified product

A series of DAP derived fatty acid amides were synthesized (**Table 2.1**) by reacting 2,6-diaminopyridine (1 mmol) with corresponding acyl chloride (1 mmol) in the presence of anhyd. triethylamine (2 mmol) and anhydrous THF (10 mL). Progress of reaction was monitored with the help of TLC. After completion of the reaction, water (1 mL) was added to quench the reaction and solvents were dried under reduced pressure. The crude mass was dissolved in ethyl acetate (10 mL) and H_2O (10 mL) and extracted with ethyl acetate (3 x 10 mL). The assorted organic extracts were dried over anhydrous Na_2SO_4, filtered and solvent was removed under reduced pressure. The native product was eluted by column chromatography using ethyl acetate-hexane (3:7) as eluents. The purity of products was examined by obtaining its spectral data.

The structure of fatty acid amide **16DAP** was confirmed by its ^{1}H NMR spectrum, where presence of broad singlet at 7.98 ppm for imine protons (-NH), whereas amine protons (-NH_2) resonated as broad singlet at 4.39 ppm. The ^{13}C NMR spectrum of the compound showed a signal peak resonated at 171.7 ppm for carbonyl carbon. The spectrum was further confirmed by its IR spectrum, which shows a strong band at 3472 cm^{-1} for amine functional group and 1666 cm^{-1} for carbonyl stretching of amide group. High resolution mass spectrum of compound **16DAP** revealed a peak at *m/z* 348.3012 $(M+H)^+$, which is consistent with support of its synthesis.

The synthesized compound **12DAP** was confirmed by its ^{1}H NMR spectrum, where presence of broad singlet at 7.86 ppm for imine protons (-NH), whereas amine protons (-NH_2) resonated as broad singlets at 4.37 ppm. The ^{13}C NMR spectrum of the compound showed a signal resonated at 171.7 ppm for carbonyl carbon. The spectrum was again confirmed by its IR spectrum, which shows a strong band at 3460 cm^{-1} for

amine functional group and 1670 cm^{-1} for carbonyl stretching of amide group. Further the compound was confirmed by its high resolution mass spectrum, which revealed a peak at *m/z* 292.2384 $(M+H)^+$.

The synthesized compound **18UDAP** was confirmed by its ^1H NMR spectrum, where presence of broad singlet at 7.94 ppm for imine protons (-NH), whereas amine protons ($-NH_2$) resonated as broad singlets at 4.33 ppm. The ^{13}C NMR spectrum of the compound showed a signal resonated at 171.7 ppm for carbonyl carbon. The spectrum was again confirmed by its IR spectrum, which shows a strong band at 3492 cm^{-1} for amine functional group and 1680 cm^{-1} for carbonyl stretching of amide group. Further the compound was confirmed by its high resolution mass spectrum, which revealed a peak at *m/z* 374.3167 $(M+H)^+$.

The synthesized compound **20DAP** was confirmed by its ^1H NMR spectrum, where presence of broad singlet at 8.29 ppm for imine protons (-NH), whereas amine protons ($-NH_2$) resonated as broad singlets at 4.43 ppm. The ^{13}C NMR spectrum of the compound showed a signal resonated at 171.7 ppm for carbonyl carbon. The spectrum was again confirmed by its IR spectrum, which shows a strong band at 3479 cm^{-1} for amine functional group and 1686 cm^{-1} for carbonyl stretching of amide group. Further the compound was confirmed by its high resolution mass spectrum, which revealed a peak at *m/z* 404.3636 $(M+H)^+$.

The synthesized compound **22DAP** was confirmed by its ^1H NMR spectrum, where presence of broad singlet at 8.27 ppm for imine protons (-NH), whereas amine protons ($-NH_2$) resonated as broad singlets at 4.35 ppm. The ^{13}C NMR spectrum of the compound showed a signal resonated at 171.9 ppm for carbonyl carbon. The spectrum

was again confirmed by its IR spectrum, which shows a strong band at 3465 cm^{-1} for amine functional group and 1664 cm^{-1} for carbonyl stretching of amide group. Further the compound was confirmed by its high resolution mass spectrum, which revealed a peak at *m/z* 432.3952 $(M+H)^+$.

2.3 Organogel preparation

A fixed amount of gelator was taken in a sample vial and added in 1 mL solvent. The vial was heated up to complete dissolution of gelator. The solution was then allowed to cool at room temperature for appropriate time (See **Table 2.2**). The state of gel was examined by inverting the glass sample vial.

2.4 Bigel preparation

A particular amount of the gelator was dissolved in 0.5 mL solvent in a sample vial and heated up to complete dissolution of gelator then immediately added 0.5 mL distilled water to the vial. The solution was then allowed to cool at room temperature for appropriate time (see Table 2). The minimum gelation concentration (MGC) was obtained by calculating minimum amount of gelator required for the formation of stable gel at room temperature. The "stable to inversion of a test tube" method was used to determine the gel state.

2.5 Thermal stability

Gel-to-sol phase transition temperature (T_{gel}) was evaluated with a tube inversion method. The gel was taken in a glass sample vial and kept in temperature controlled oil bath at 20^oC. The temperature of hot plate was increased by 1^oC after every one minute. The temperature at which viscous gel breaks down was esteemed as T_{gel}.

2.6 Scanning electronic microscopy (SEM)

The bigels and organogels were deep freeze dried under lyophilisation and morphology analysis was carried out with the SEM EVO18 Zeiss model.

2.7 Drug loading

A fixed amount of gelator (**22DAP**) was added to 1 mL of solvent (DMSO) at their MGC and heated to form a clear solution. Then a weighed amount of ibuprofen was added to the clear gelator solution at 70 ^{o}C. The solution was mixed thoroughly and allowed to cool at temperature 20^{o}C for 1h. The amount of ibuprofen was increased up to stable gel formation achieved and drug loading was calculated by using the following equation.[54]

$$\text{Drug loading content (\%)} = \frac{\text{Weight of the drug in organogel}}{\text{Weight of organogel}} \times 100 \quad \text{.....eq. 1}$$

2.8 Drug release study

pH-responsive drug release from the ibuprofen composite gel was studied at pH 5.5 and 7.4, respectively. Accordingly, ibuprofen encapsulated gel was placed at room temperature for 2h to attain the equilibrium then buffer solution of pH 5.5 was added and mixed thoroughly. The degradation pattern of gel was examined at pH 5.5 by obtaining the absorbance at 264 nm in kinetic absorption study. In the same way degradation pattern of gel was also examined at pH 7.4.

2.9 Results and discussion

We have synthesized five derivatives of fatty acid amide gelators (**12DAP**, **16DAP**, **18UDAP**, **20DAP** and **22DAP**) for this study using DAP as a linker and alkyl chains of

varying lengths. The products were obtained in good to excellent yields (see **Table 2.1**). It was observed that when the length of alkyl chain of fatty acids increases, selective mono-acylation occurs and corresponding products were obtained exclusively (entries 4 and 5, **Table 2.1**).

Gelation of above fatty acid amide gelators were studied in various solvent systems by heating-cooling method. Initially, efforts were made to solubilize the fatty acid amide (**16DAP**) in water, but it was insoluble even upon heating. Then we have tried to dissolve **16DAP** in polar solvents such as methanol and DMSO, and observed that it appeared as clear solution at room temperature. In spite of that it was heated and then cooled to room temperature, which did not afford organogel. We have next focused our study towards screening co-solvent system and accordingly methanol and water mixture were used in 1:1 ratio (10 mg/mL) and heated to 50^{o}C to obtain a clear solution. The resulting clear solution was allowed to cool to room temperature under ambient conditions for 5-10 minutes which afforded white solid aggregates at the bottom of the sample vial. Bigel formation was confirmed by stable-to-inversion of the test tube method (**Figure 2.1**).[52]

Further a relative study of **16DAP** gelator was performed in various solvent-water mixtures (1:1 ratio) and the obtained results are summarized in **Table 2.2**. This study gave clear evidence that methanol-water combination should be a good choice for self-assembling of fatty acid amides for aggregation.

After establishing the optimal gelating conditions, next we were interested in exploring the effect of alkyl chains on the gelation behaviour. Accordingly, the length of fatty acid alkyl chain was reduced from sixteen (**16DAP**) to twelve carbon (**12DAP**), but did not yield such a promising results and bigel formation occurred only after 24 h cooling the vial at ambient temperature. However, upon increasing the length of fatty acid amides

(**20DAP** and **22DAP**), the bigel formation happened instantly which demonstrates that the stability of bigels are directly dependent on the length of fatty acid alkyl chains because of increasing the strength of van der Wall forces.[43]

Table 2.2: Bigelation/organogelation study of DAP derived fatty acid amides in various solvent systems

Gelater	Solvent *(v/v; 1 mL)*	Gel	Gelation time	MGC (mg/mL)	T_{gel} (K)[a]
16DAP	DMSO	No	-	-	-
"	$CH_3OH:H_2O$ (1:1)	Yes	<5 min	10	338
"	$C_2H_5OH:H_2O$	Yes	5 min	10	337
"	DMF : water	No	-	-	-
"	DMSO : water	Yes	10 min	10	334
"	DCM : water	No	-	-	-
"	ethylacetate : water	No	-	-	-
"	acetonitrile : water	Yes	10 min	10	336
"	hexane : water	No	-	-	-
12DAP	$CH_3OH:H_2O$ (1:1)	Yes	24h	10	300
"	DMSO	No	-	-	-
20DAP	$CH_3OH:H_2O$ (1:1)	Yes	<5 min	10	350
"	DMSO	No	-	-	-
"	CH_3OH	Yes	30-45 min	10	302
22DAP	$CH_3OH:H_2O$ (1:1)	Yes	<5 min	10	356
"	DMSO	Yes[b]	15-30 min	5	309
"	CH_3CN	Yes[c]	30 min	5	310
"	CH_3OH	Yes[c]	30 min	5	313
18UDAP	$CH_3OH:H_2O$ (1:1)	Yes	3-4 days	10	-
"	DMSO	No	-	-	-
12BDAP	$CH_3OH:H_2O$ (1:1)	No	-	-	-
"	DMSO	No	-	-	-

[a]Tube Inversion Method; [b]Transparent gel; [c]Opaque gel;
MCG = minimum gelation concentration; T_{gel} = Gel-to-sol phase transition temperature

Furthermore, fatty acid amides having unsaturation (**18UDAP**) were also screened for its gelation ability which hardly produced bigel after 3-4 days at 20 ^oC. This phenomenon

can be explained by the fact that saturated fatty acid tails pack closely together, causing them to be solid at room temperature whereas unsaturated fatty acids cannot pack closely together resulting relatively low melting points and turned up liquid at room temperature (**Figure 2.1**).

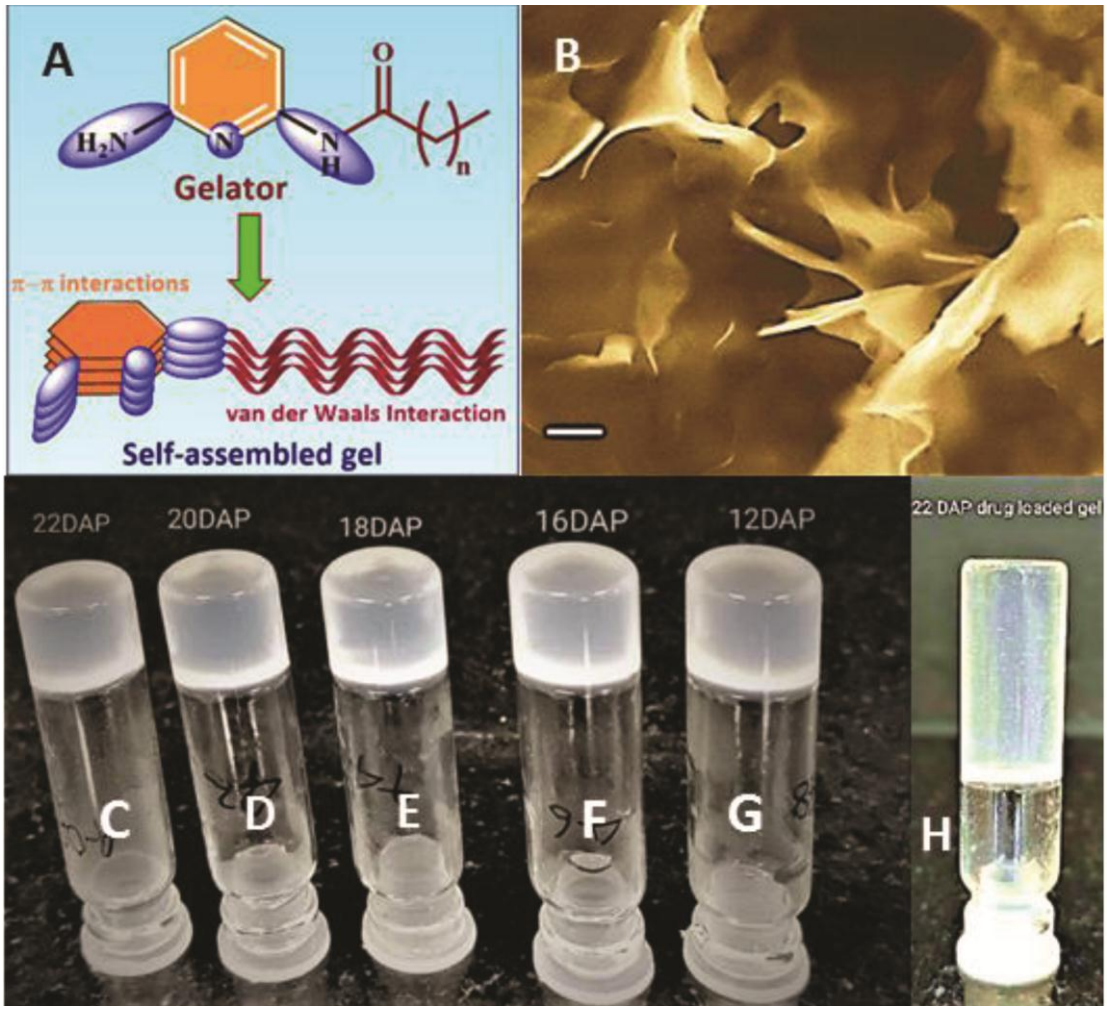

Figure 2.1. (**A**) Proposed packing model for the self-assembled gel.[52] (**B**) SEM image of bigel of **16DAP**in 1:1 MeOH-H_2O mixture (image recorded for xerogel; scale bar = 1 µM); Photograph of vials showing gelation of fatty acid amides gelators; bigel in 1:1 MeOH-H_2O mixture (**C-G**). **C** = **22DAP**; **D** = **20DAP**; **E** = **16DAP**; **F** = **12DAP**; **G** = **18UDAP**; **H** = **22DAP** (organogel formed in DMSO).

Finally we have studied the concentration ratio of MeOH-H_2O mixture at which the bigel formation (**16DAP**) occurs and results are presented in **Table 2.3**.

Table 2.3: Ability of bigel formation of fatty acid amide gelator (16DAP) in different ratios of CH_3OH-H_2O mixture

Gelater (10 mg/mL)	Methanol:Water *(v/v)*	Gel	Description	Gelation time
16DAP	10:90	No	milky suspension	-
	20:80	Yes	white gel	15-20 min
	30:70	Yes	white gel with a little excess solvant	<5 min
	40:60	Yes	white gel with no excess solvant	<5 min
	50:50	Yes	white gel with no excess solvant	<5 min
	60:40	Yes	white gel with no excess solvant	<5 min
	70:30	Yes	white gel with no excess solvant	10-15 min
	80:20	Yes	clear solution converted into white gel	10-15 min
	90:10	Yes	clear solution converted into white gel	30-45 min

With the ability of these fatty acid amides to produce bigels, we expanded our investigation to screen the ability of organogel formation of longer saturated fatty acid amides in various polar organic solvents such as MeOH, DMSO and acetonitrile, surprisingly **20DAP** and **22DAP** afforded organogel with MeOH (opaque gel), however, only **22DAP** produced transparent gel in DMSO. A detailed study of solvents systems for the study of bi- and organogelation ability is presented in **Table 2.2.**

Bigels are more stable as compared to organogels and its thermal stability T_{gel} (K) was determined by inverted-tube method.[53] In relative study, the T_{gel} of **12DAP**, **16DAP**, **20DAP** and **22DAP** was measured at 1% w/v of gelator and results are appeared in **Table 2.2,** which suggests that with increase in the aliphatic side chain of fatty acid amide gelators, thermal stability of gels simultaneously got enhanced due to increased strength of Van der wall forces.[54] These bigels are stable for more than six months at 25-30^{o}C. The organogel of **22DAP** organogel (DMSO) was stable at room temperature

but not at higher temperature. Further it was also observed that **22DAP** organogel was deformed on heating and reversibly formed again on cooling, and stability was checked by tube-inversion method (**Table 2.2**).[53]

Morphology of xerogels

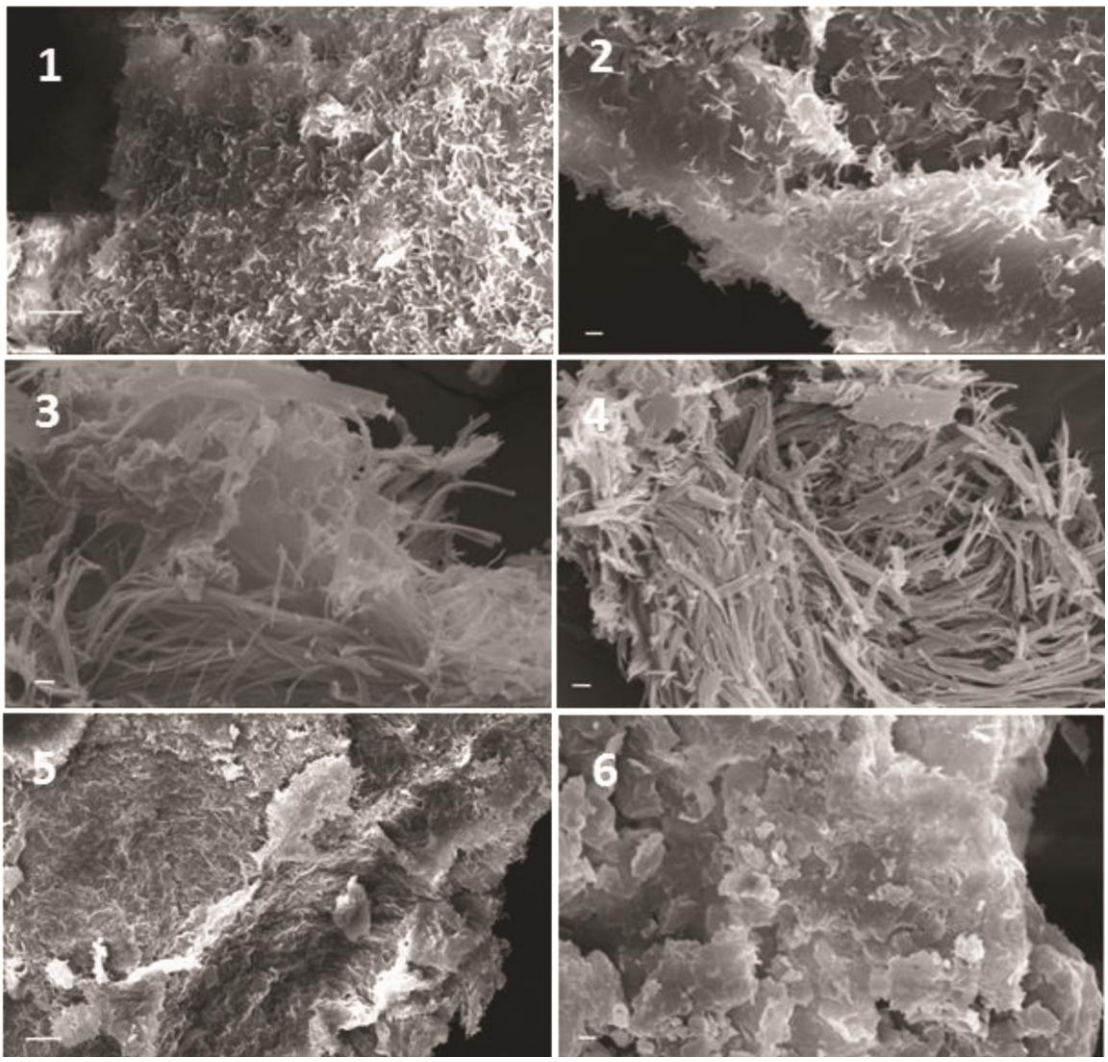

Figure 2.2. SEM images of xerogels: **22DAP** (1 and 2; Sacle Bar 10 µM and 2 µM); 20DAP (3 and 4; Scale Bar = 2 µM); **16DAP** (5 and 6; Sacle Bar 10 µM and 2 µM).

The mechanism and the forces that drive the formation of self-assembled morphologies is not clearly understood. FAA (fatty acid amide) gelators possesses the DAP moiety and it is likely that the π - π interactions between the pyridine

groups provide the required rigidity and also play a major role in directing the aggregation. The morphology of self-assembled freeze dried (xerogel) bigels and organogels were characterized by the Scanning Electron Microscopy (SEM) imaging techniques. Xerogels were prepared by removal of water and solvent from bigels using freeze drying technique. The morphologies for xerogels (**22DAP**, **20DAP** and **16DAP**) are given in **Figure 2.2**. The SEM images revealed that bigels were self-assembled into a collection of flower bunch and vein like structures, respectively (**Figure 2.2**).

2.10 Drug incorporation and pH-responsive release

Earlier methods reported that self-assembly derived from chemically modified prodruggelators and drug loaded thermo-responsive hydrogels were involved in drug delivery processes.[53] Since prodrugs were prepared by covalent linkage of drug molecules with gelators, there could be high possibility of losing the original activity of drug during chemical modification of gelator while its release which makes this process limited for drug delivery applications. Diaminopyridine derivatives are known to have a lower tendency to dimerise and can recognize and bind to ligands through hydrogen bonding.[55] These results imply that drug (ibuprofen) encapsulation in organogels can occur through the hydrogen bond network and not by any chemical modification that may be released by the action of a pH dependent degradation method.

In this study ibuprofen, a non-steroidal anti-inflammatory drug (NSAID), was taken as the model drug which is known to be a best-quality hydrophobic drug consisting of

a large hydrophobic part comprised of an aromatic ring and a carbon tail and a small hydrophilic head, where the oxygen groups are located. The drug composite gel was found to be transparent and the amount of entrapped ibuprofen in **22DAP** organogel was 6.78% (percentage of drug loading was calculated by equation 1) in 0.5% w/v, which indicates high degree of encapsulation. The SEM morphologies of xerogel (**22DAP**) contained ibuprofen (**8** and **9**) are given in **Figure 2.3**.

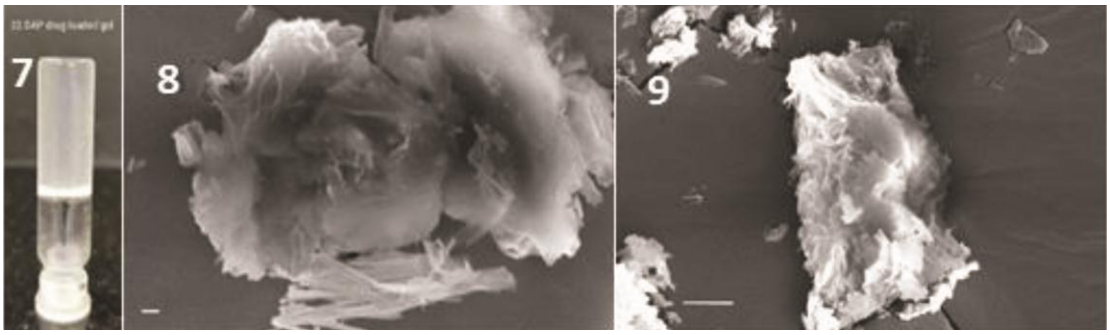

Figure 2.3. Photograph of drug loaded gel (**7**); SEM images of xerogel **22DAP** (organogel in DMSO) contained ibuprofen (**8**-**9**) Scale bar (**8**) = 2 µM; Scale bar (**9**) = 10µM.

2.11 Fourier transmission infrared spectroscopy (FT-IR) analysis

The FT-IR spectra of ibuprofen (**a**); xerogel (**b**); and ibuprofen drug composite xerogel (**c**), are given in **Figure 2.4**. In the spectrum of native xerogel (**b**), there are characteristic peaks at 3288 and 3164 cm^{-1}, which are attributed to NH bond stretching of NH_2. The peaks at 2918 and 2850 cm^{-1} corresponds to CH stretching of alkyl chains whereas peaks at 1673 cm^{-1} corresponds to the stretching vibration of amide carbonyl >C=O and other characteristic peaks of xerogel are 2375, 2313, 716 and 710 cm^{-1}. Ibuprofen drug consist a strong peak at 1714 cm^{-1} which corresponds to the stretching vibration frequency of acid carbonyl >C=O functionality while other characterstic peaks are at 2912, 2860, 1459, 1415, 1371, 864 and 514 cm^{-1} (**a**). FT-IR

spectra of drug composite xerogel (**c**) had band at 1701 and 1660 cm^{-1}, respectively relative to the stretching of the acid carbonyl >C=O of ibuprofen and stretching vibration of amide carbonyl C=O of native xerogel, respectively. The other peaks are at 2912, 2860, 1459, 1415, 1371, 864 and 514 cm^{-1} which are relative to the characteristic peaks of ibuprofen drug while the peaks 2375, 2313, 716 and 710 cm^{-1} are relative to the peaks of xerogel. From **Figure 2.4**, it is clear that drug composite xerogel contains the characteristic peaks of both the drug and native xerogel, while absence of peaks at 3289 and 3169 cm^{-1}, which are attributed to NH bond stretching frequencies of NH_2 support that NH_2 is involved in H-bonding during drug composite gel. It has been observed that during gel preparation, **22DAP** forms a stable gel at neutral pH while gets precipitated at pH < 7.

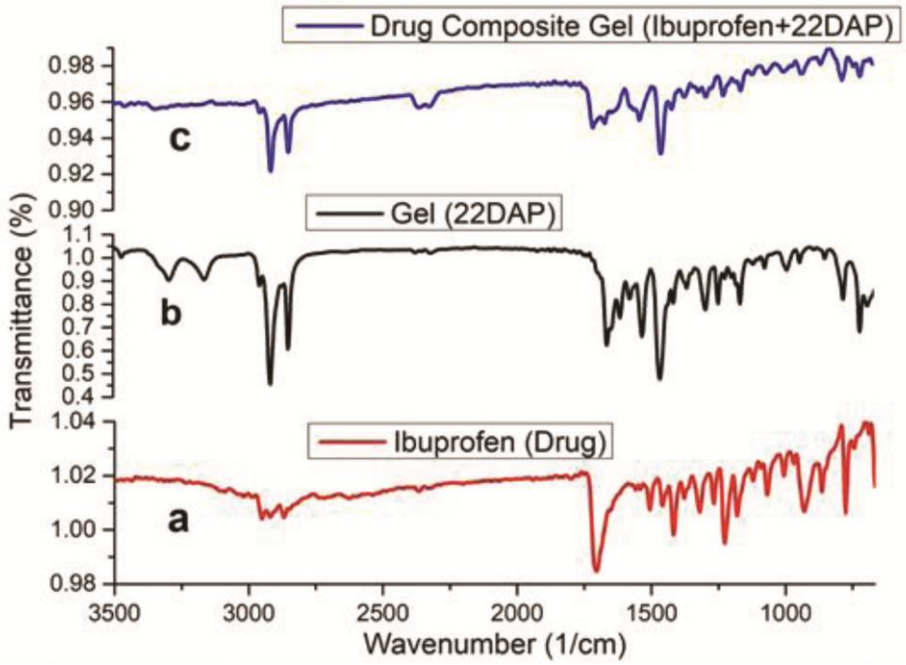

Figure 2.4. FT-IR spectra (**a**) ibuprofen drug; (**b**) Organogel (**22DAP**); (**c**) ibuprofen drug composite organogel.

This behaviour shows that the terminal amine group play important role in the self-assembling process by the formation hydrogen-bonding networks. The pH effect on the degradation of gel could also be observed by the naked eye.

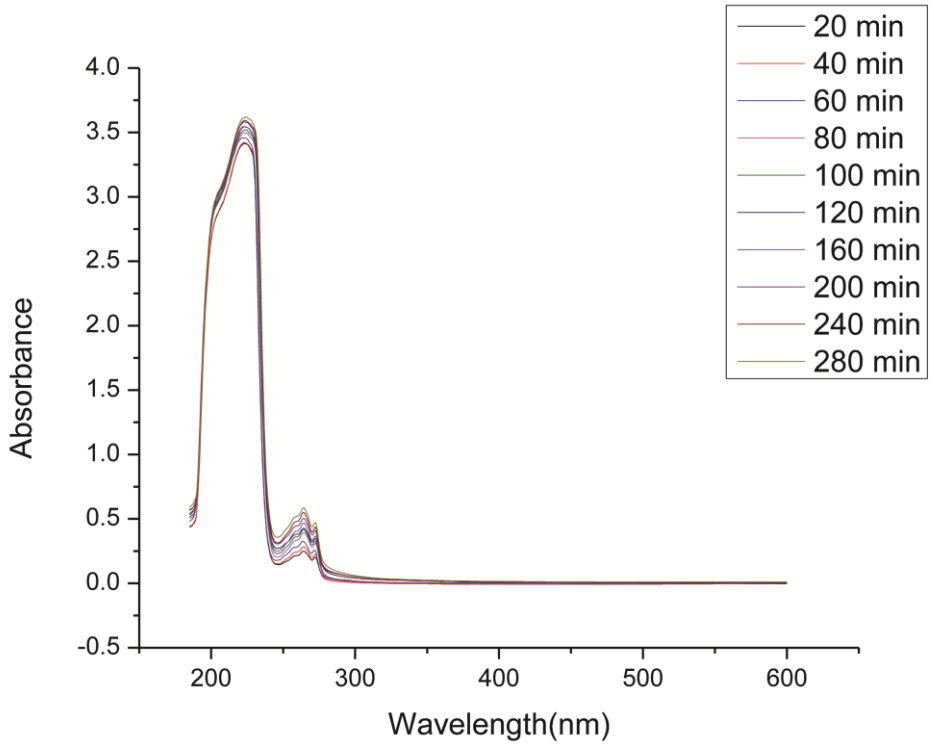

Figure 2.5. UV spectra of kinetic degradation of drug composite organogels at pH 5.5.

2.12 Comparative pH sensitive release: Kinetics of ibuprofen drug from organogel

The release kinetics of drug composite organogel was systematically investigated using hydrophobic ibuprofen at pH 5.5 and 7.4, respectively.[3a] The pH responsive gel degradation of the **22DAP** gelator was useful to encapsulate the drug in organogel and later release by changing the pH of the medium.[56] The release behavior of ibuprofen was initially investigated on gelator's MGC at pH 5.5. At a particular interval of time 100 µL of supernatant solution was taken out and diluted it to 3 mL and then filtered. The absorbance at 264 nm was measured for each sample and the concentration of

ibuprofen that was released from the organogel was obtained. The kinetic degradation profile of the drug composite organogel was recorded by UV absorption spectroscopy (**Figure 2.5**).

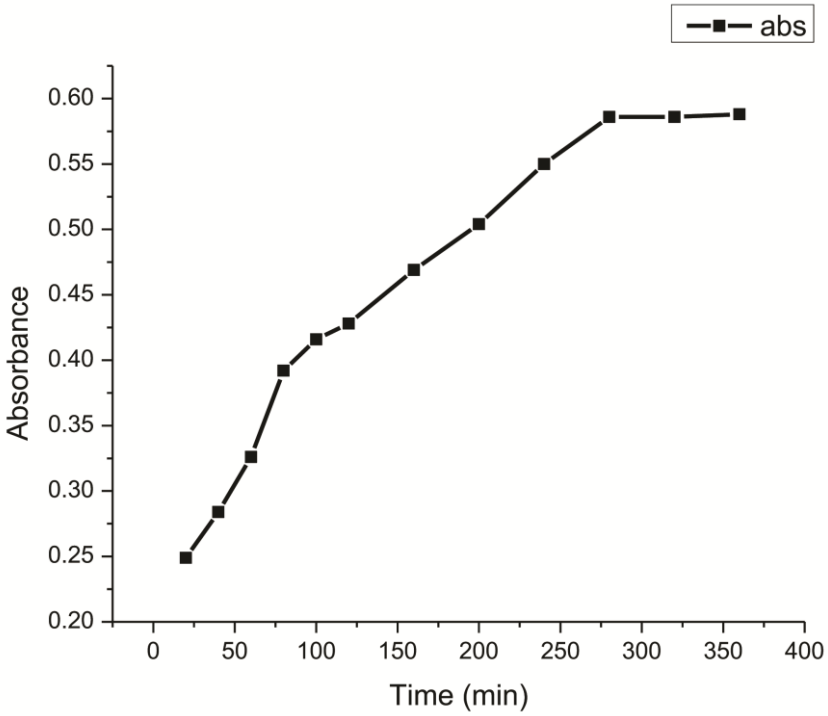

Figure 2.6. pH-Responsive cumulative release of ibuprofen from the ibuprofen composite organogels at pH 5.5.

The pH responsive cumulative release of ibuprofen from the ibuprofen composite organogel was shown in **Figure 2.6** which indicates that there was no more release of the drug observed after 280 minutes.

In case of pH 7.4, only 35% drug was released from drug composite gel in 360 minutes and no more release was observed after 360 minutes as ibuprofen has bulky molecular structure leading to slower transmission through the porous channel of gel at neutral pH (7.4). The kinetic degradation profile of the drug composite organogel was recorded by UV absorption spectroscopy (**Figure 2.7**).

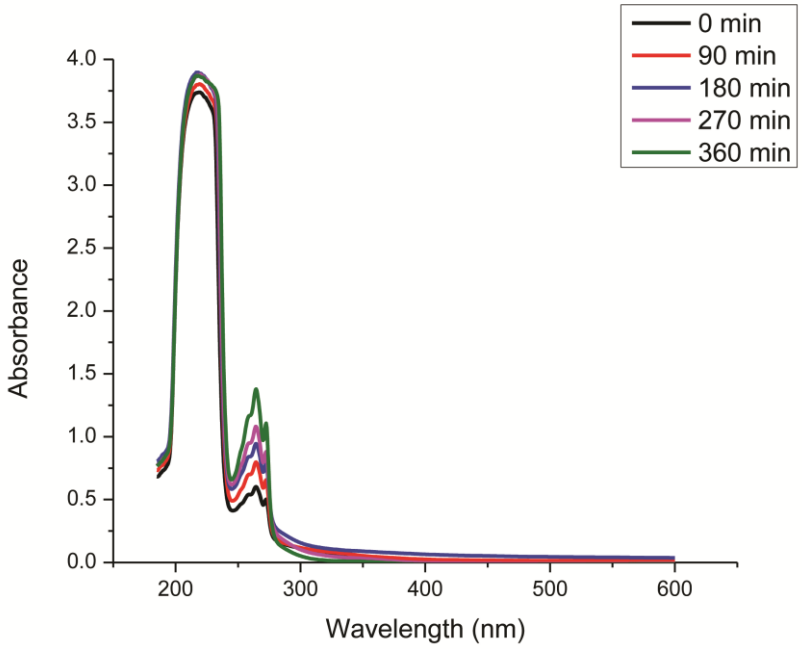

Figure 2.7. UV spectra of kinetic degradation of drug composite organogels at pH 7.4.

The pH responsive cumulative release of ibuprofen from the ibuprofen composite organogel was shown in **Figure 2.8** which indicates that there was no more release of the drug observed after 360 minutes in case of slightly basic buffer having pH (7.4).

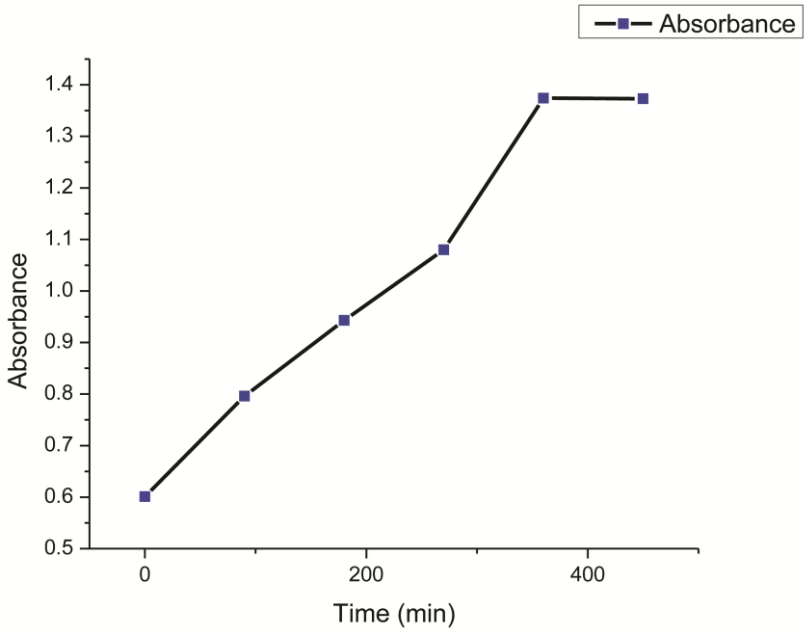

Figure 2.8. pH-Responsive cumulative release of ibuprofen from the ibuprofen composite organogels at pH 7.4.

However, in case of acidic pH (5.5), the release % of ibuprofen was increased upto 57% in 280 minutes and no more release was observed afterwards. In case of acidic pH (5.5) both the release amount and release rate were increased because of the weakening of π-π stacking and H-bonding interactions. These results were reproduced twice.

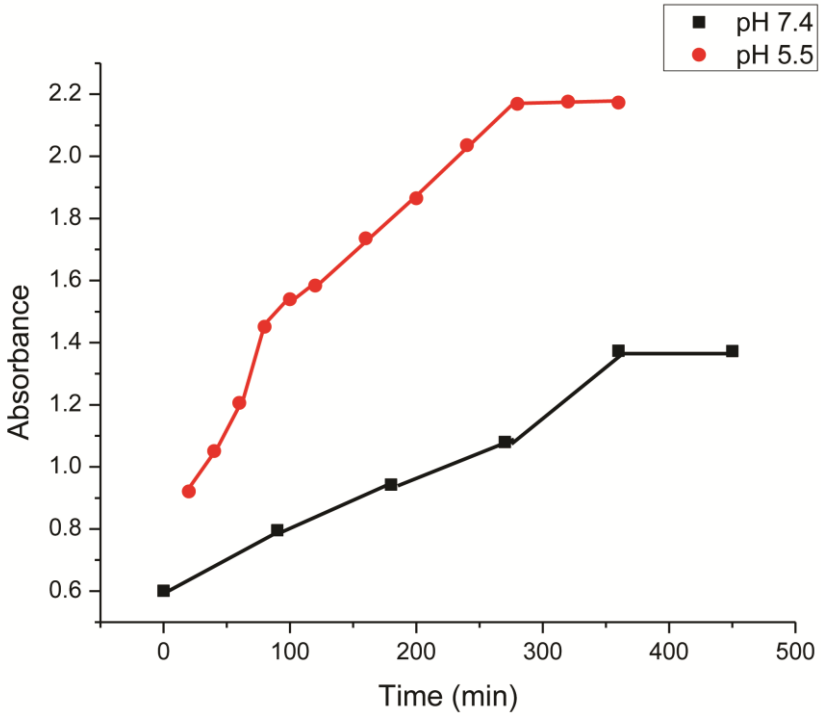

Figure 2.9. pH-Responsive cumulative release of ibuprofen from the ibuprofen composite organogels at pH 7.4 (black line) and pH 5.5 (red line).

2.13 Conclusion

In summary, DAP derived low molecular weight fatty acid amides were synthesized using standard organic procedures. Further, these gelators self-assembled in water-solvent mixture and polar organic solvents and formed bi and organogel, respectively. The analogues having saturated long aliphatic chains formed stable bigels while unsaturated analogues hardly afforded bigels. Stability of bigels increases with increase

in the length of saturated fatty acid alkyl chain. Incubation technique concluded that bigels are thermally more stable as compared to organogels. The minimum gelation concentration of organic gel is 0.5% w/v which behaves like a super gelators. The prepared gel emulsion encapsulated and released the drug molecule ibuprofen at ambient temperature without altering the structure and activity. The results reported here offer an opportunity in the field of pharmaceuticals to use these analogues as drug carrier vehicles.

2.14 Experimental

2.14.1 Materials

Ibuprofen and analytical grade solvents were purchased fromSigma Aldrich. 2,6-Diaminopyridine, lauric acid, palmitoyl chloride, oleic acid, arachidic acid, behenic acid, oxalyl chloride and triethyl amine were purchased from Central Drug House and used as such. Distillation of solvents was done before its use.

2.14.2 Methods

Nuclear Magnetic Resonance (NMR) spectra (^{1}H) and (^{13}C) were recorded on Bruker 400 MHz and 101 MHz spectrometer, respectively. The samples were made in chloroform-d or DMSO-d^{6} using tetramethylsilane (TMS) as the internal standard and chemical shift values were measured in ppm on a scale downfield from TMS and the coupling constant *J* are in Hz. The molecular masses of synthesized compounds were obtained by high resolution LC-MS (Agilent) instrument. The UV-visible absorption spectra were obtained with a Shimadzu UV Vis spectrophotometer. The IR spectra were obtained with FT-IR Bruker Instrument.

***N*-(6-Aminopyridin-2-yl)palmitamide (16DAP)**

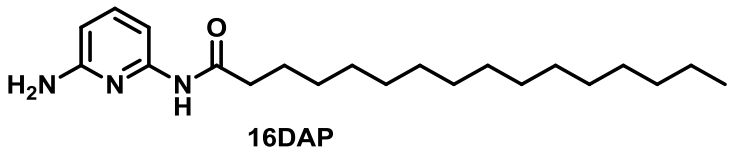

16DAP

Yield = 81%; Off-white solid, m. p. = 73°C; IR (Neat): υ_{max} 3472, 3302, 3154, 2956, 2917, 2849, 2375, 2317, 1666, 1614, 1577, 1527, 1564, 1414, 1288, 1247, 1163 cm^{-1}; ^{1}H NMR (400 MHz, Chloroform-*d*) δ 7.98 (s, 1H, N**H**), 7.56 (d, *J* = 8.0 Hz, 1H, Ar-**H**), 7.45 (t, *J* = 7.9 Hz, 1H, Ar-**H**), 6.24 (d, *J* = 7.9 Hz, 1H, Ar-**H**), 4.39 (s, 2H, -N**H$_2$**), 2.32 (t, *J* = 7.6 Hz, 2H, -C**H$_2$**CO-), 1.68 (p, *J* = 7.4 Hz, 2H, -C**H$_2$**CH$_2$CO-), 1.29-1.26 (m, 24H, Aliphatic proton), 0.89 (t, *J* = 6.6 Hz, 3H, -C**H$_3$**); ^{13}C NMR (101 MHz, Chloroform-*d*) δ 171.7 (1C, NH**C**=O), 157.1 (1C, Ar-**C**), 149.9 (1C, Ar-**C**), 140.2 (1C, Ar-**C**), 104.1 (1C, Ar-**C**), 103.3 (1C, Ar-**C**), 37.8 (1C, -CO**C**H-), 31.9, 29.7, 29.7, 29.7, 29.7, 29.6, 29.6, 29.5, 29.4, 29.2, 29.2, 25.5, 22.7 (peaks for **13C**), 14.1 (1C, -**C**H$_3$) ;HRMS (ESI) calcd. for $C_{21}H_{37}N_3O$: 348.3009 $(M+H)^+$. Found 348.3012.

***N*-(6-Aminopyridin-2-yl)dodecanamide (12DAP)**

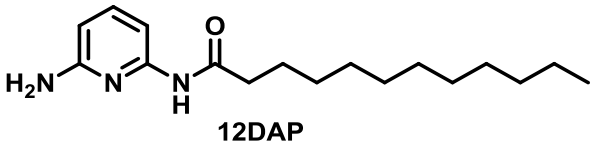

12DAP

Yield = 75%; Off-white solid, m. p. = 65°C; IR (Neat): υ_{max} 3460, 3236, 3198, 2951, 2919, 2846, 2374, 2323, 1670, 1606, 1581, 1538, 1449, 1410, 1292, 1247, 1155 cm^{-1}; ^{1}H NMR (400 MHz, Chloroform-*d*) δ 7.86 (s, 1H, N**H**), 7.56 (d, *J* = 7.9 Hz, 1H, Ar-**H**), 7.46 (t, *J* = 7.9 Hz, 1H, Ar-**H**), 6.25 (d, *J* = 7.9 Hz, 1H, Ar-**H**), 4.37 (s, 2H, -N**H$_2$**), 2.33

(t, *J* = 7.6 Hz, 2H, -C**H**$_2$CO-), 1.69 (p, *J* = 7.4 Hz, 2H, -C**H**$_2$CH$_2$CO-), 1.31-1.26 (m, 16H, Aliphatic proton), 0.89 (t, *J* = 6.7 Hz, 3H, -C**H**$_3$); ^{13}C NMR (101 MHz, Chloroform-*d*) δ 171.7 (1C, NH**C**=O), 157.0 (1C, Ar-**C**), 149.9 (1C, Ar-**C**), 140.2 (1C, Ar-**C**), 104.2 (1C, Ar-**C**), 103.3 (1C, Ar-**C**), 37.8 (1C, -CO**C**H-), 31.9, 29.6, 29.5, 29.4, 29.4, 29.3, 29.2, 25.4, 22.7 (peaks for **9C**), 14.1 (1C, -**C**H$_3$); HRMS (ESI) calcd. for $C_{17}H_{29}N_3O$: 292.2383 $(M+H)^+$. Found 292.2384.

***N*-(6-Aminopyridin-2-yl)oleamide** (**18UDAP**)

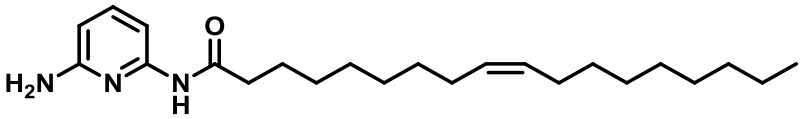

18UDAP

Yield = 79%; Yellow viscous liquid; IR (Neat): υ_{max} 3492, 3321,3205, 3059, 3003, 2919, 2853, 2370, 2315, 1680, 1616, 1577, 1536, 1451, 1348, 1293, 1247, 1156cm^{-1}; ^{1}H NMR (400 MHz, $CDCl_3$) δ 7.94 (s, *J* = 10.0 Hz, 1H, N**H**), 7.47 (d, *J* = 8.1 Hz, 1H, Ar-**H**), 7.36 (t, *J* = 7.9 Hz, 1H, Ar-**H**), 6.16 (d, *J* = 7.9 Hz, 1H, Ar-**H**), 5.26 (s, 1H, olefinic proton), 5.25 (dd, *J* = 24.1, 12.0 Hz, 1H, olefinic proton), 4.33 (s, 2H, -N**H**$_2$), 2.24 (t, *J* = 7.6 Hz, 2H, -C**H**$_2$CO-), 1.94 (dq, *J* = 12.7, 6.4, 5.9 Hz, 4H, -C**H**$_2$CH=CHC**H**$_2$-), 1.60 (p, *J* = 7.4 Hz, 2H, -C**H**$_2$CH$_2$CO-), 1.22 – 1.19 (m, 20H, Aliphatic proton), 0.80 (t, *J* = 6.6 Hz, 3H, -C**H**$_3$); ^{13}C NMR (101 MHz, Chloroform-*d*) δ 171.7 (1C, NH**C**=O), 157.0 (1C, Ar-**C**), 149.8 (1C, Ar-**C**), 140.3 (1C, Ar-**C**), 130.0, 129.7 (2C,unsaturated), 104.1 (1C, Ar-**C**), 103.3 (1C, Ar-**C**), 37.8 (1C, -CO**C**H-), 31.9, 29.8, 29.7, 29.6, 29.5, 29.3, 29.3, 29.2, 29.1, 27.2, 27.2, 25.4, 22.7 (peaks for **13C**), 14.1 (1C, -**C**H$_3$); HRMS (ESI) calcd. for $C_{23}H_{39}N_3O$: 373.3166 $(M+H)^+$. Found 374.3167.

***N*-(6-Aminopyridin-2-yl)icosanamide (20DAP)**

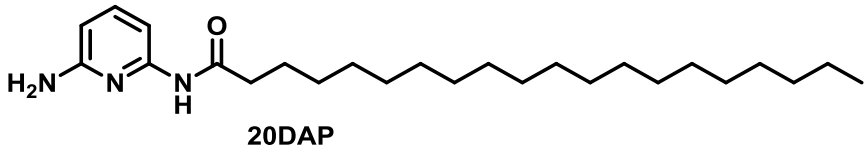

20DAP

Yield = 87%; Off-white solid, m. p. = 85°C; IR (Neat): υ_{max} 3479, 3282, 3168, 2956, 2915, 2849, 2376, 2313, 1686, 1614, 1573, 1531, 1461, 1414, 1367, 1288, 1247, 1163 cm^{-1}; ^1H NMR (400 MHz, Chloroform-*d*) δ 8.29 (s, 1H, N**H**), 7.59 (d, *J* = 8.0 Hz, 1H, Ar-**H**), 7.48 (t, *J* = 8.0 Hz, 1H, Ar-**H**), 6.26 (d, *J* = 7.9 Hz, 1H, Ar-**H**), 4.43 (s, 2H, -N**H**$_2$), 2.37 (t, *J* = 7.5 Hz, 2H, -C**H**$_2$CO-), 1.72 (p, *J* = 7.5 Hz, 2H, -C**H**$_2$CH$_2$CO-), 1.34-1.27 (m, 32H, Aliphatic proton), 0.90 (t, *J* = 6.5 Hz, 3H, -C**H**$_3$); ^{13}C NMR (101 MHz, Chloroform-*d*) δ 171.7 (1C, NH**C**=O), 156.7(1C, Ar-**C**), 149.6 (1C, Ar-**C**), 140.6 (1C, Ar-**C**), 104.2 (1C, Ar-**C**), 103.3 (1C, Ar-**C**), 37.8 (1C, -CO**C**H-), 31.9, 29.7, 29.7, 29.7, 29.7, 29.6, 29.6, 29.6, 29.6, 29.6, 29.5, 29.5, 29.4, 29.4, 29.2, 25.4, 22.7 (peaks for **17C**), 14.1 (1C, -**C**H$_3$); HRMS (ESI) calcd. for $C_{25}H_{45}N_3O$: 404.3635 $(M+H)^+$. Found 404.3636.

***N*-(6-Aminopyridin-2-yl)docosanamide (22DAP)**

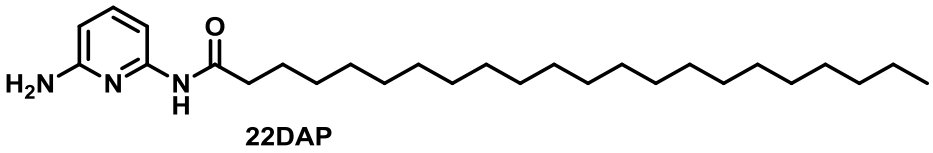

22DAP

Yield = 90%;Off-white solid, m. p. = 87°C; IR (Neat): υ_{max} 3465, 3288, 3164, 2952, 2914, 2849, 2375, 2313, 1664, 1614, 1579, 1530, 1466, 1414, 1363, 1294, 1249, 1165 cm^{-1}; ^1H NMR (400 MHz, Chloroform-*d*) δ 8.27 (s, 1H, N**H**), 7.51 – 7.19 (m, 2H, Ar-**H**), 6.17 (d, *J* = 7.9 Hz, 1H, Ar-**H**), 4.35 (s, 2H, -N**H**$_2$), 2.29 (t, *J* = 7.5 Hz, 2H, -

C**H$_2$**CO-), 1.63 (p, *J* = 7.3 Hz, 2H, -C**H$_2$**CH$_2$CO-), 1.23-1.18 (m, 36H, Aliphatic proton), 0.81 (t, *J* = 6.6 Hz, 3H, -C**H$_3$**); ^{13}C NMR (101 MHz, Chloroform-*d*) δ 171.9 (1C, NH**C**=O), 156.7(1C, Ar-**C**), 149.6 (1C, Ar-**C**), 140.7 (1C, Ar-**C**), 104.2 (1C, Ar-**C**), 103.3 (1C, Ar-**C**), 37.8 (1C, -CO**C**H-), 31.9, 29.7, 29.7, 29.6, 29.6, 29.6, 29.6, 29.6, 29.6, 29.6, 29.6, 29.5, 29.5, 29.4, 29.2, 29.2, 25.4, 22.7 (peaks for **19C**), 14.1 (1C, -**C**H$_3$); HRMS (ESI) calcd. for $C_{27}H_{49}N_3O$: 432.3948 $(M+H)^+$. Found 432.3952.

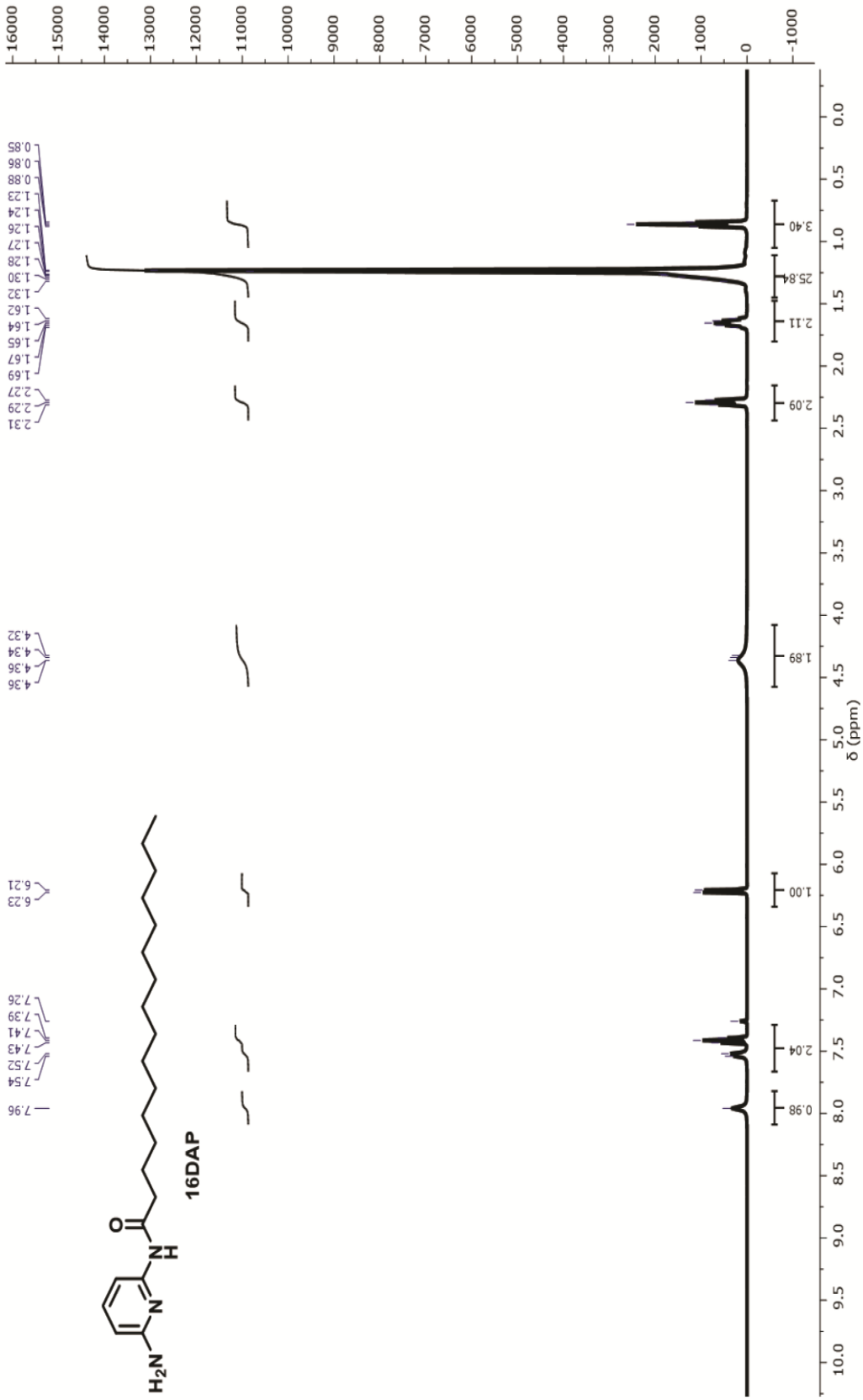

Figure 2.10. ^{1}H NMR spectrum of **16DAP** in $CDCl_3$ (400 MHz)

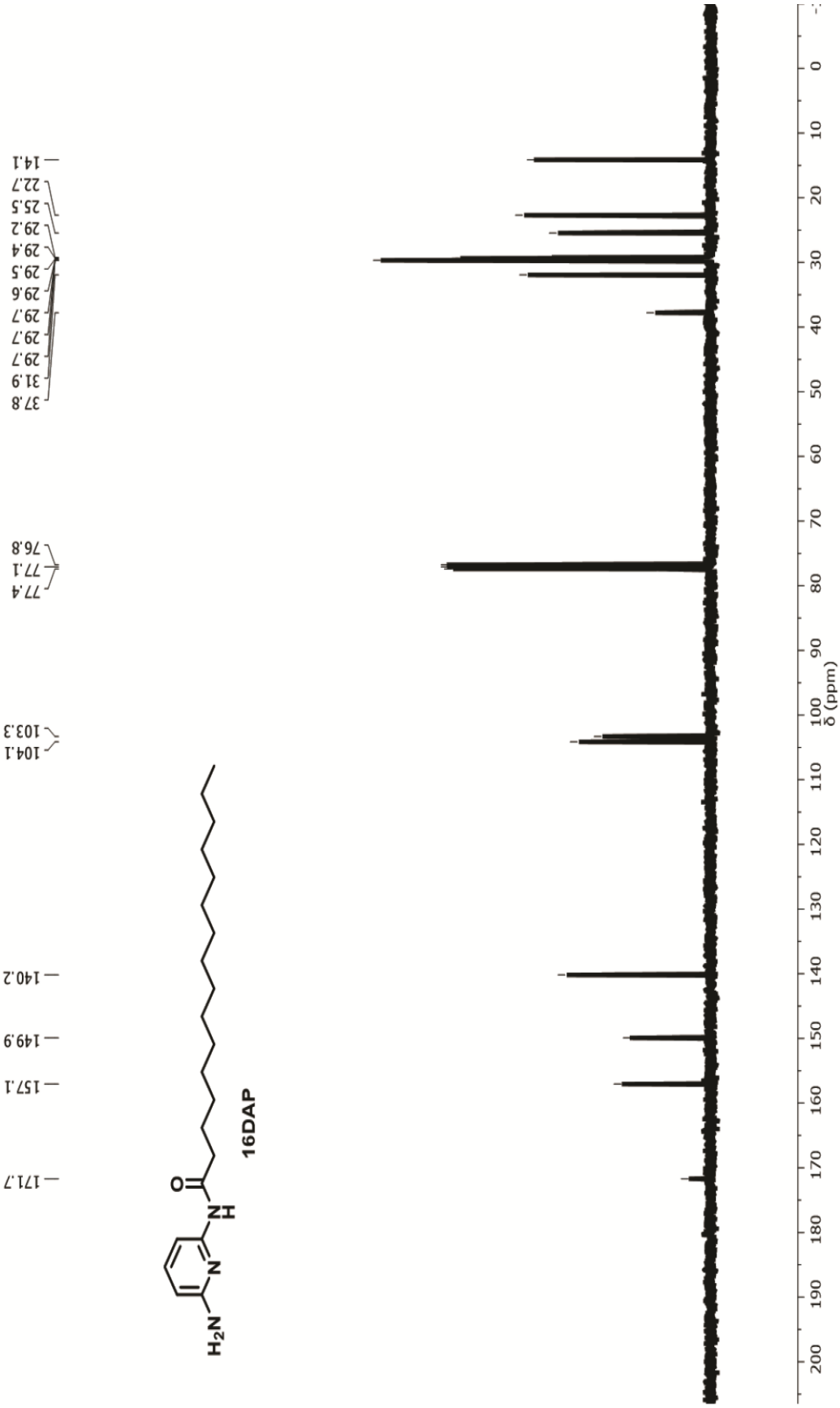

Figure 2.11. ^{13}C NMR spectrum of **16DAP** in $CDCl_3$ (100 MHz)

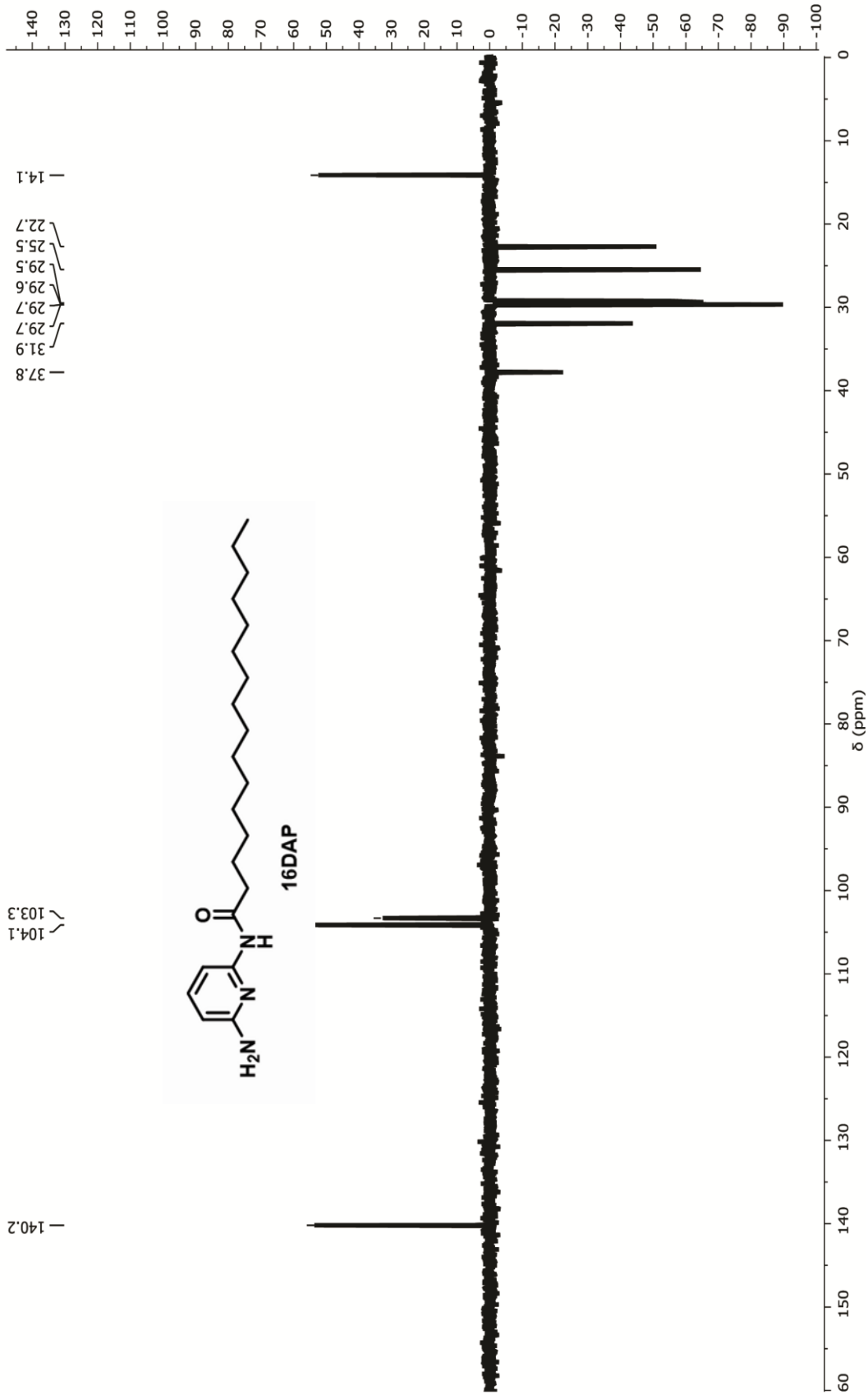

Figure 2.12. ^{13}C NMR (Dept-135) spectrum of **16DAP** in $CDCl_3$ (100 MHz)

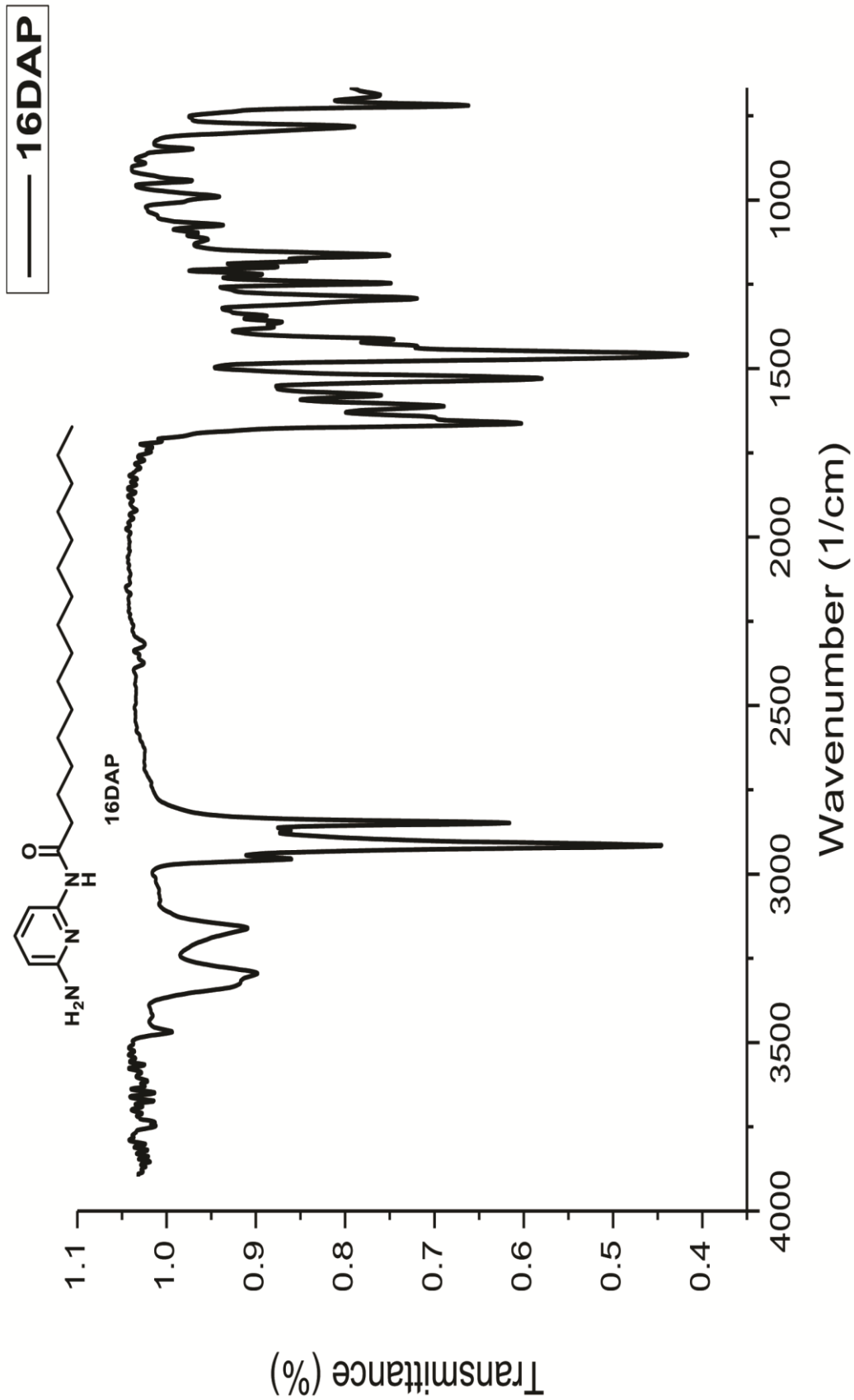

Figure 2.13. IR spectrum of **16DAP**

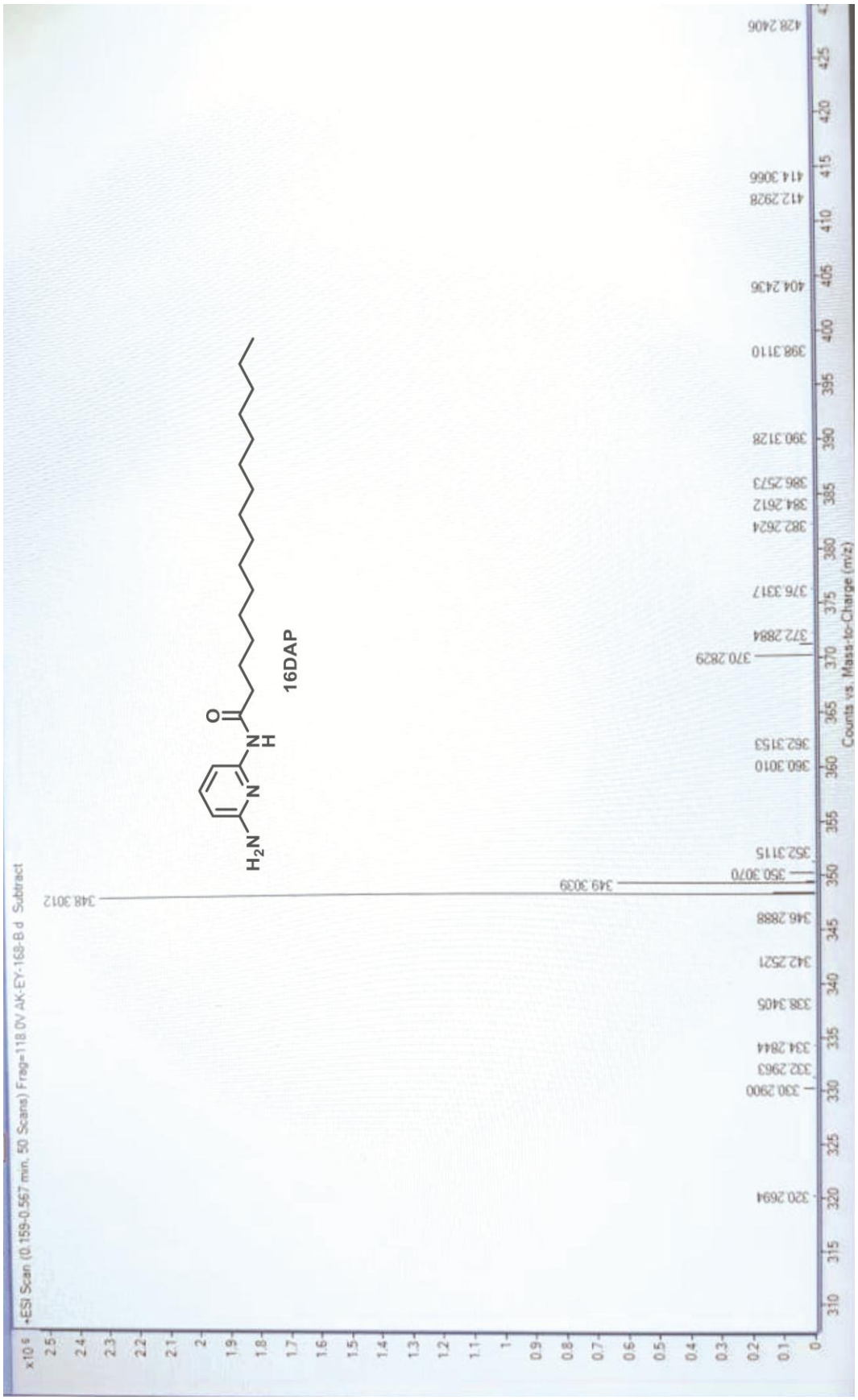

Figure 2.14. High resolution mass spectrum (HRMS) of **16DAP**

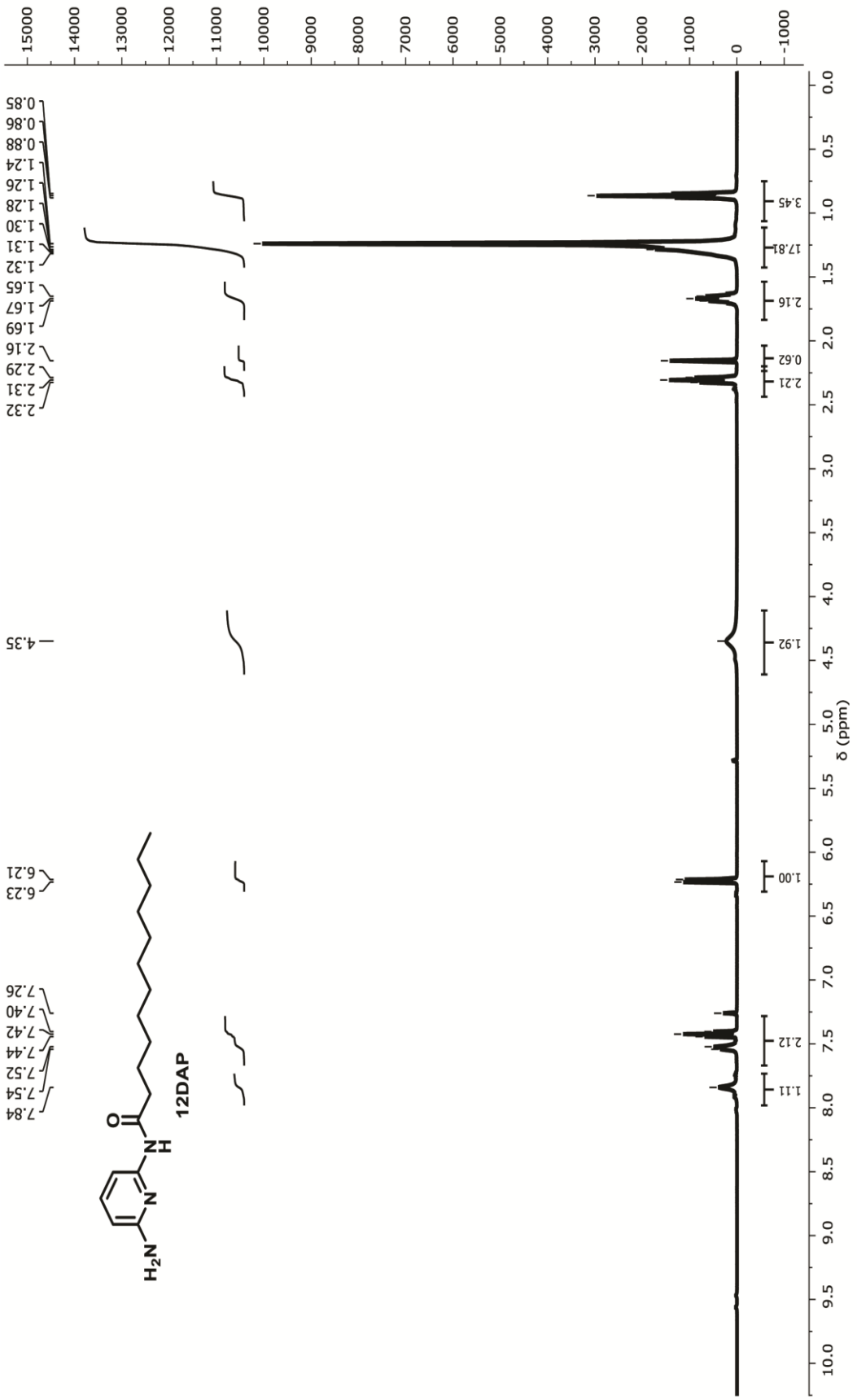

Figure 2.15. ^{1}H NMR spectrum of **12DAP** in $CDCl_3$ (400 MHz)

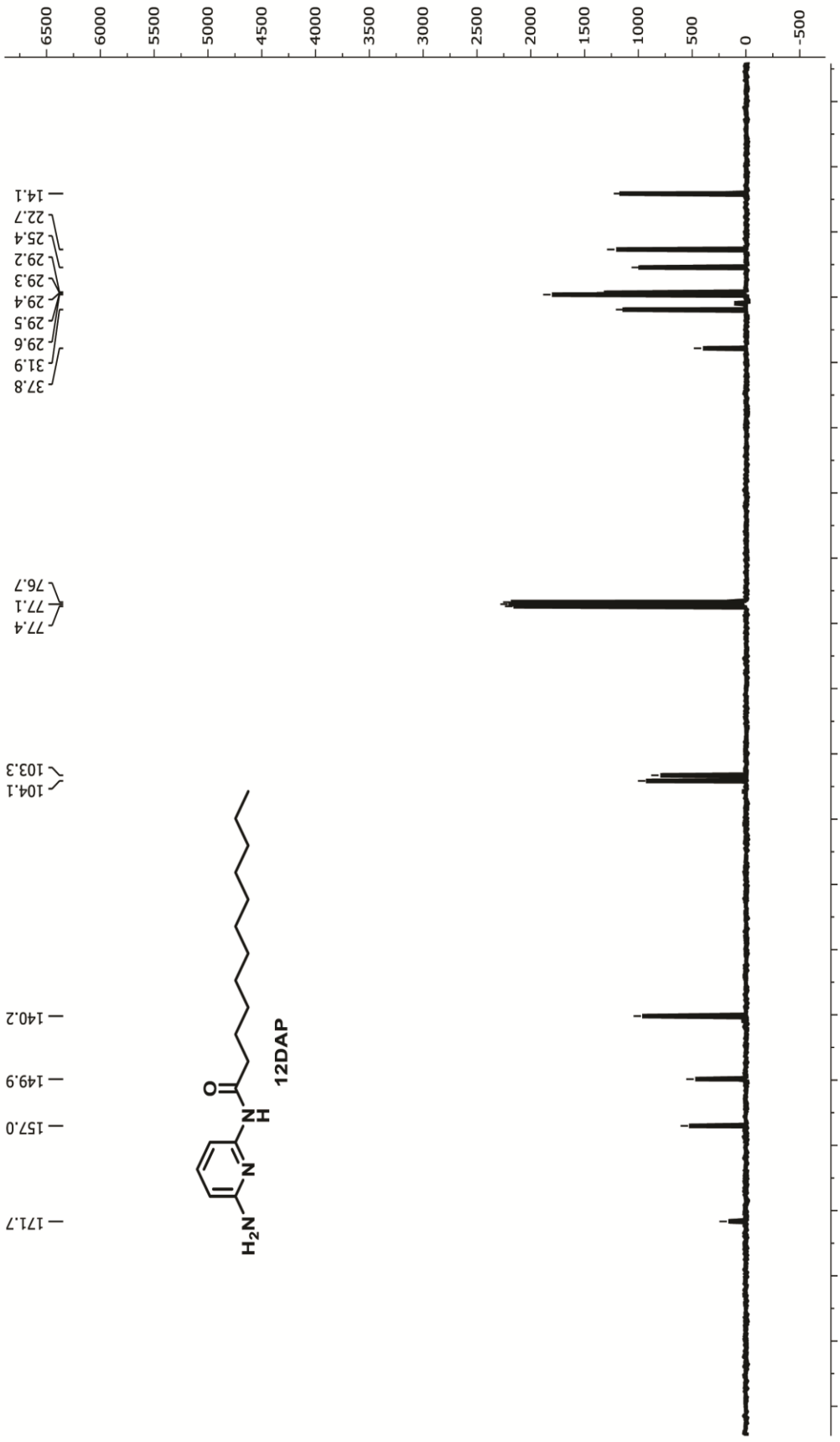

Figure 2.16. ^{13}C NMR spectrum of **12DAP** in $CDCl_3$ (100 MHz)

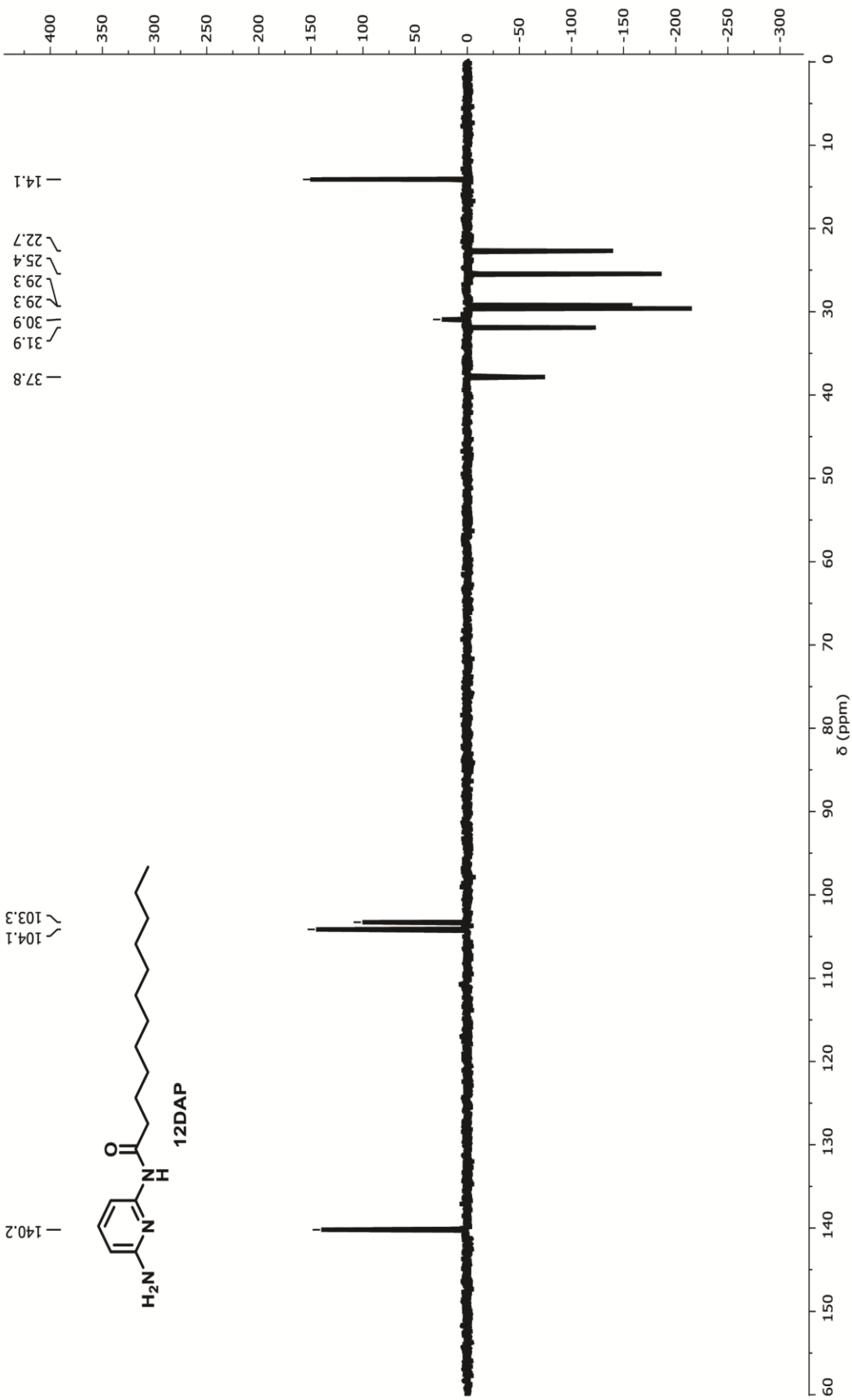

Figure 2.17. ^{13}C NMR (Dept-135) spectrum of **12DAP** in $CDCl_3$ (100 MHz)

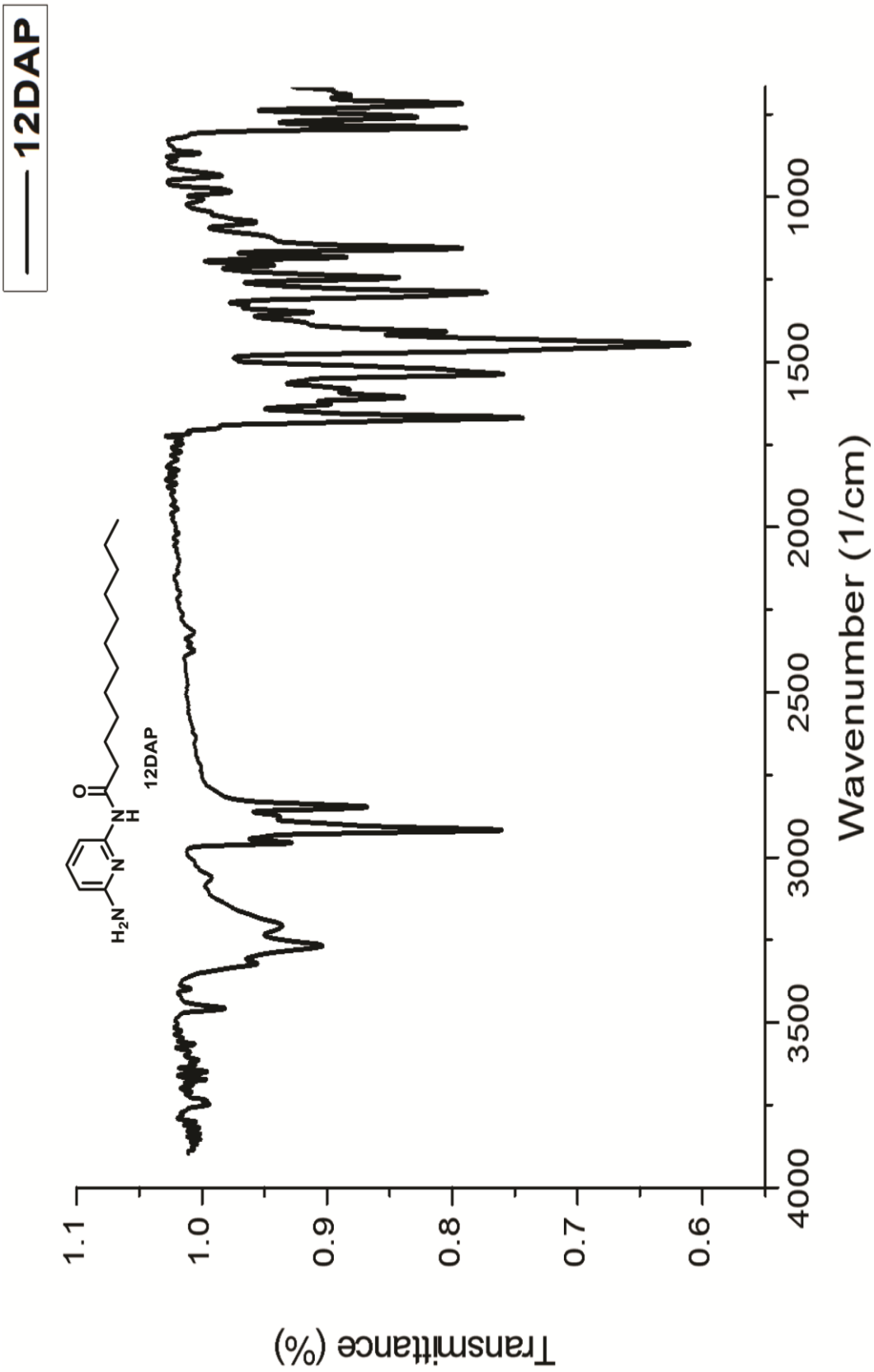

Figure 2.18. IR spectrum of **12DAP**

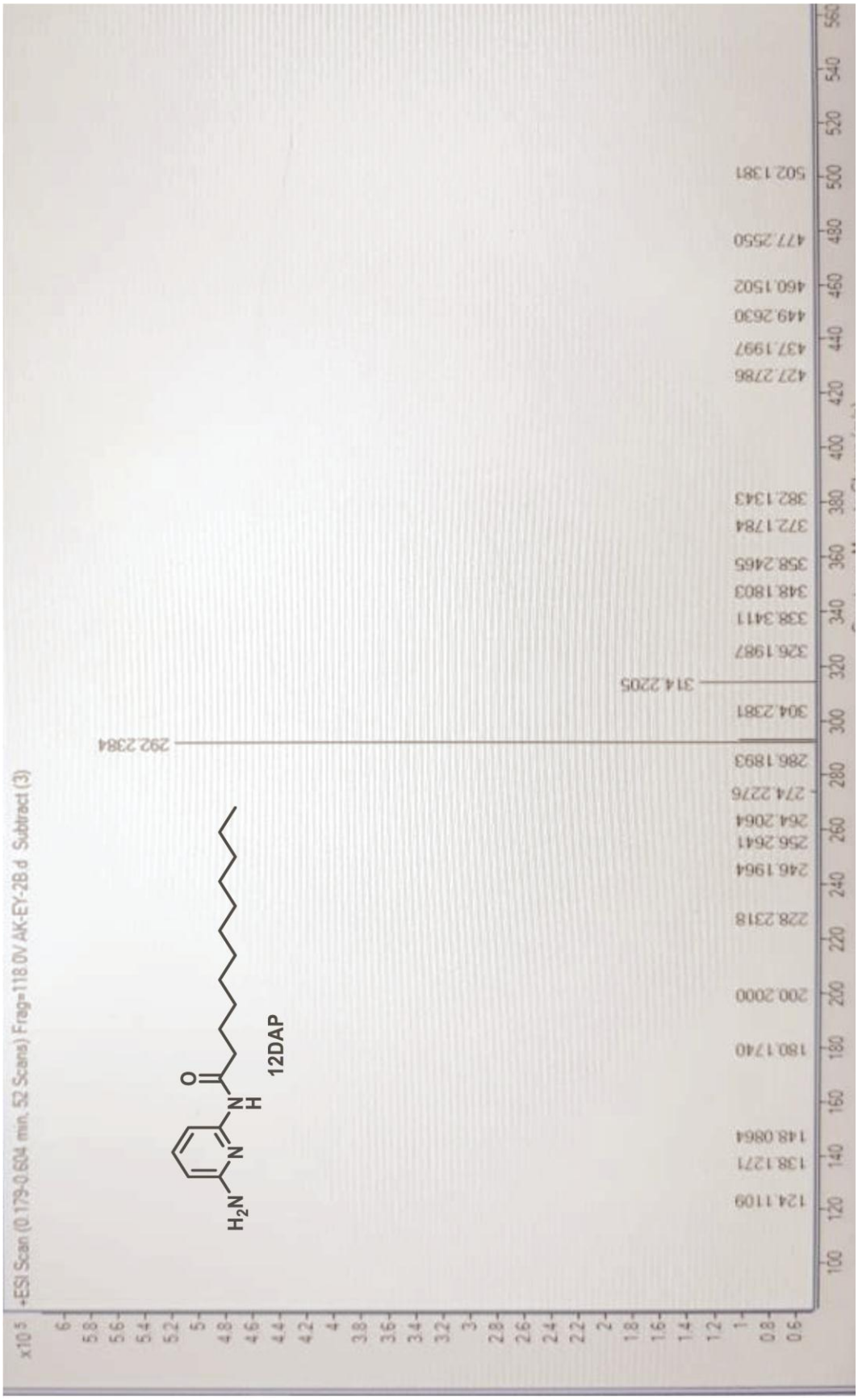

Figure 2.19. High resolution mass spectrum (HRMS) of **12DAP**

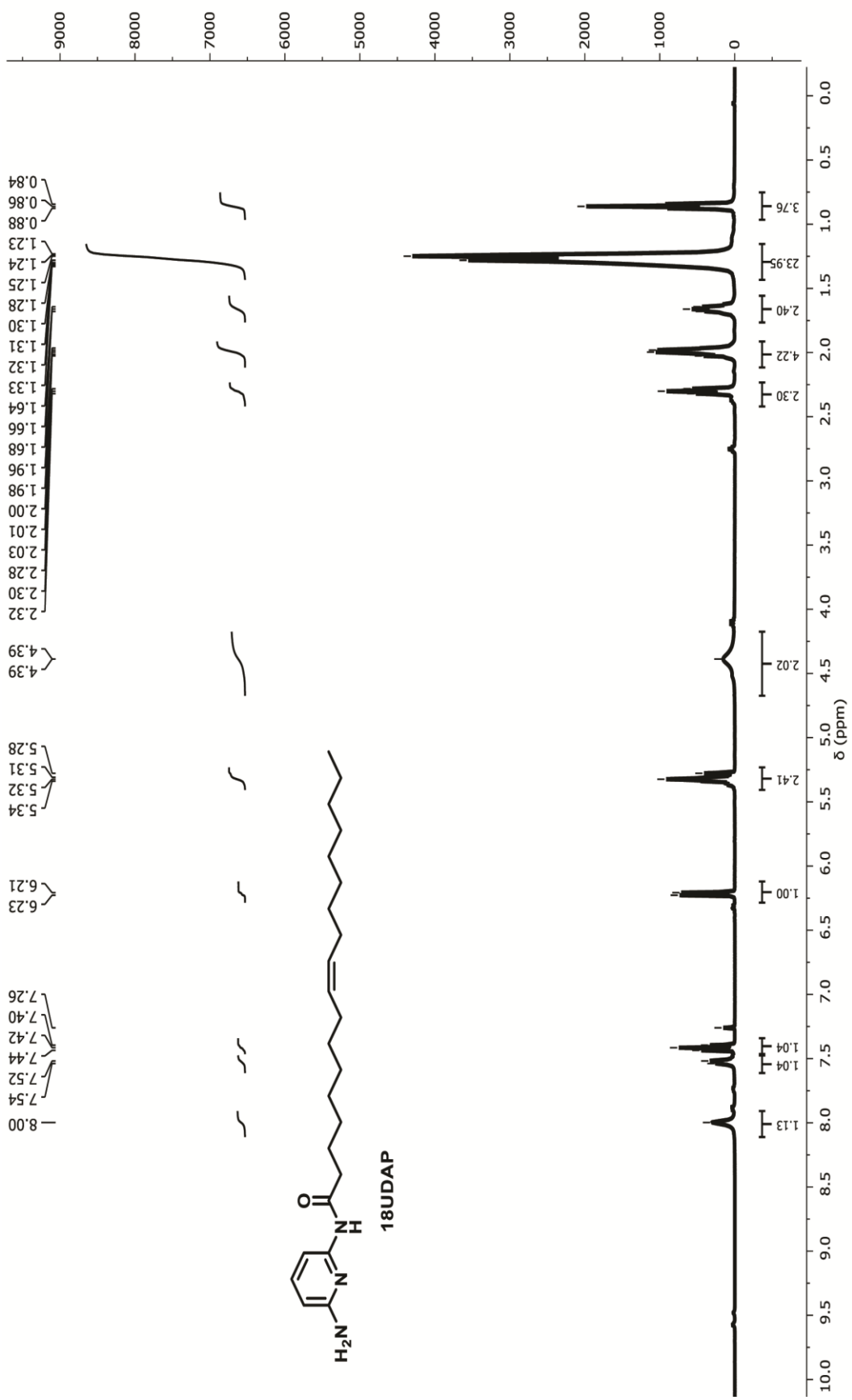

Figure 2.20. ^{1}H NMR spectrum of **18UDAP** in $CDCl_3$ (400 MHz)

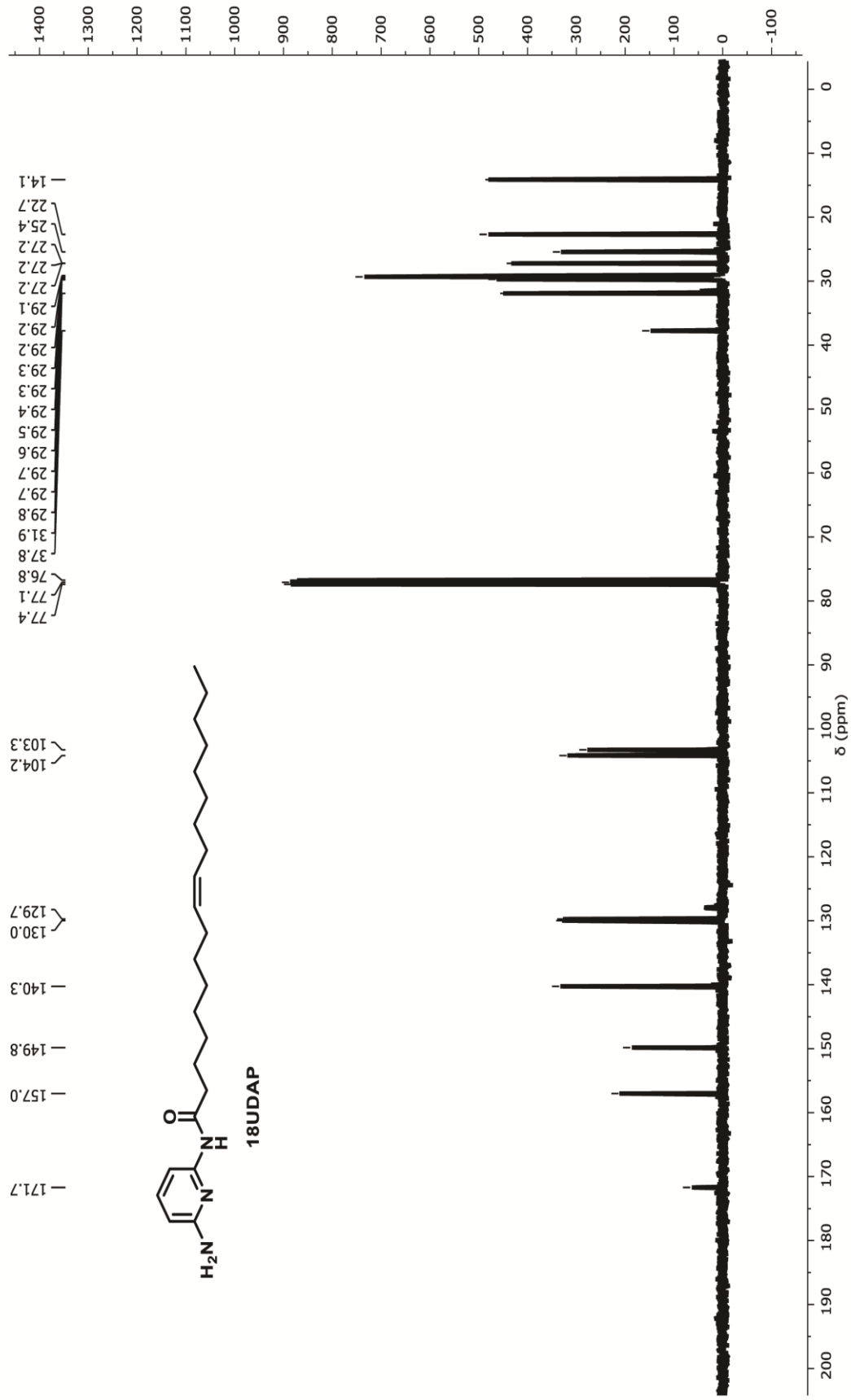

Figure 2.21. ^{13}C NMR spectrum of **18UDAP** in $CDCl_3$ (100 MHz)

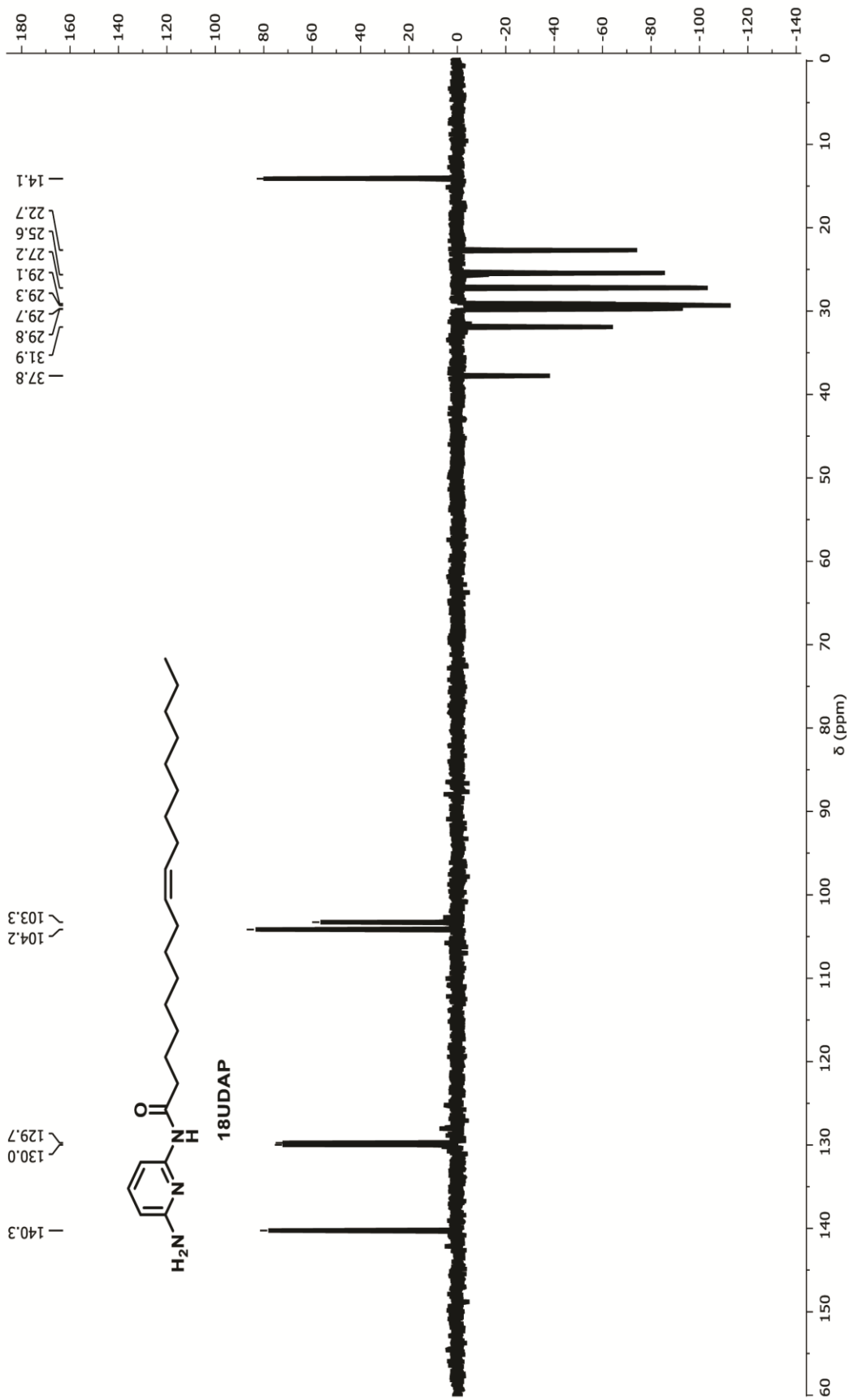

Figure 2.22. ^{13}C NMR (Dept-135) spectrum of **18UDAP** in $CDCl_3$ (100 MHz)

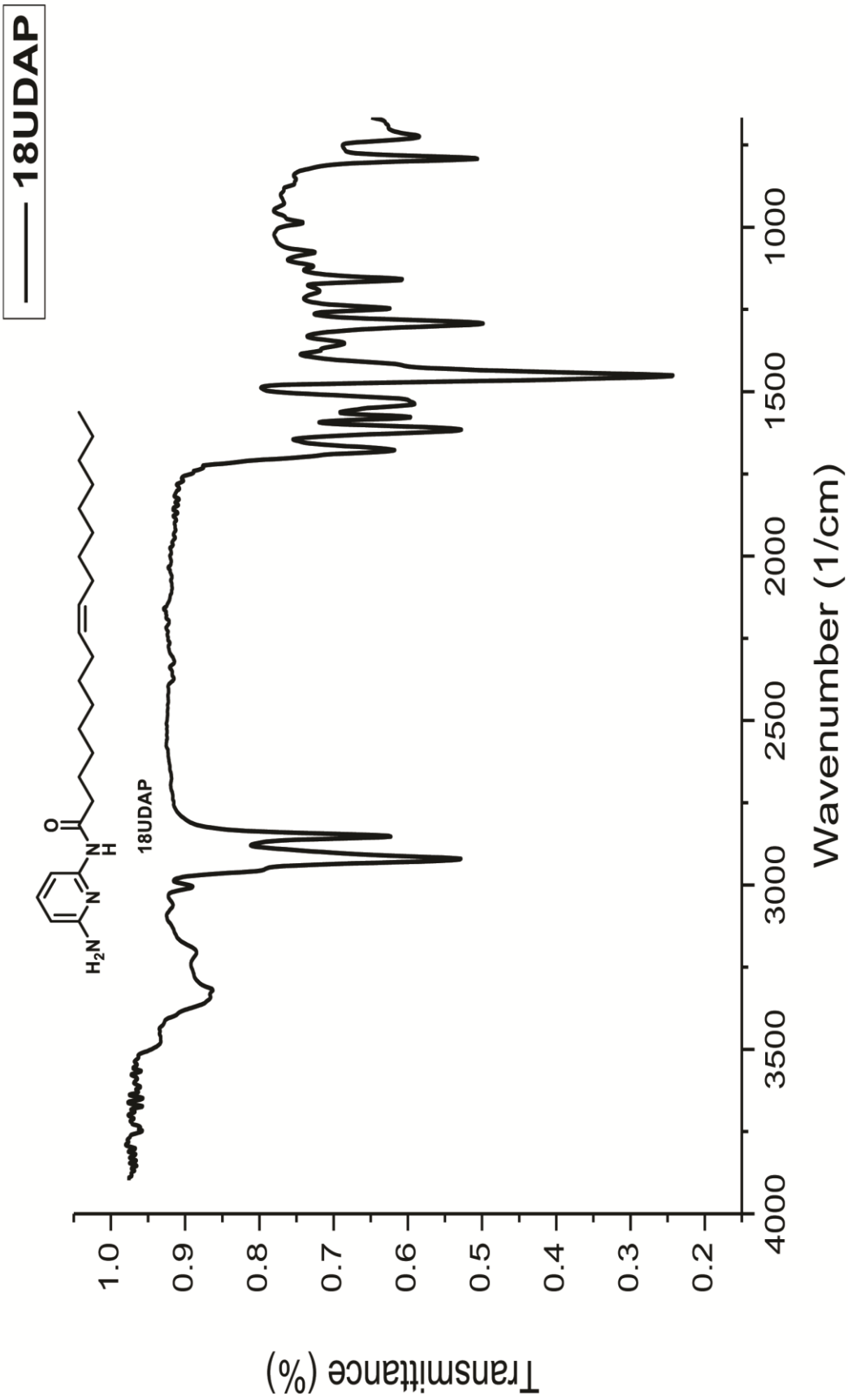

Figure 2.23. IR spectrum of **18UDAP**

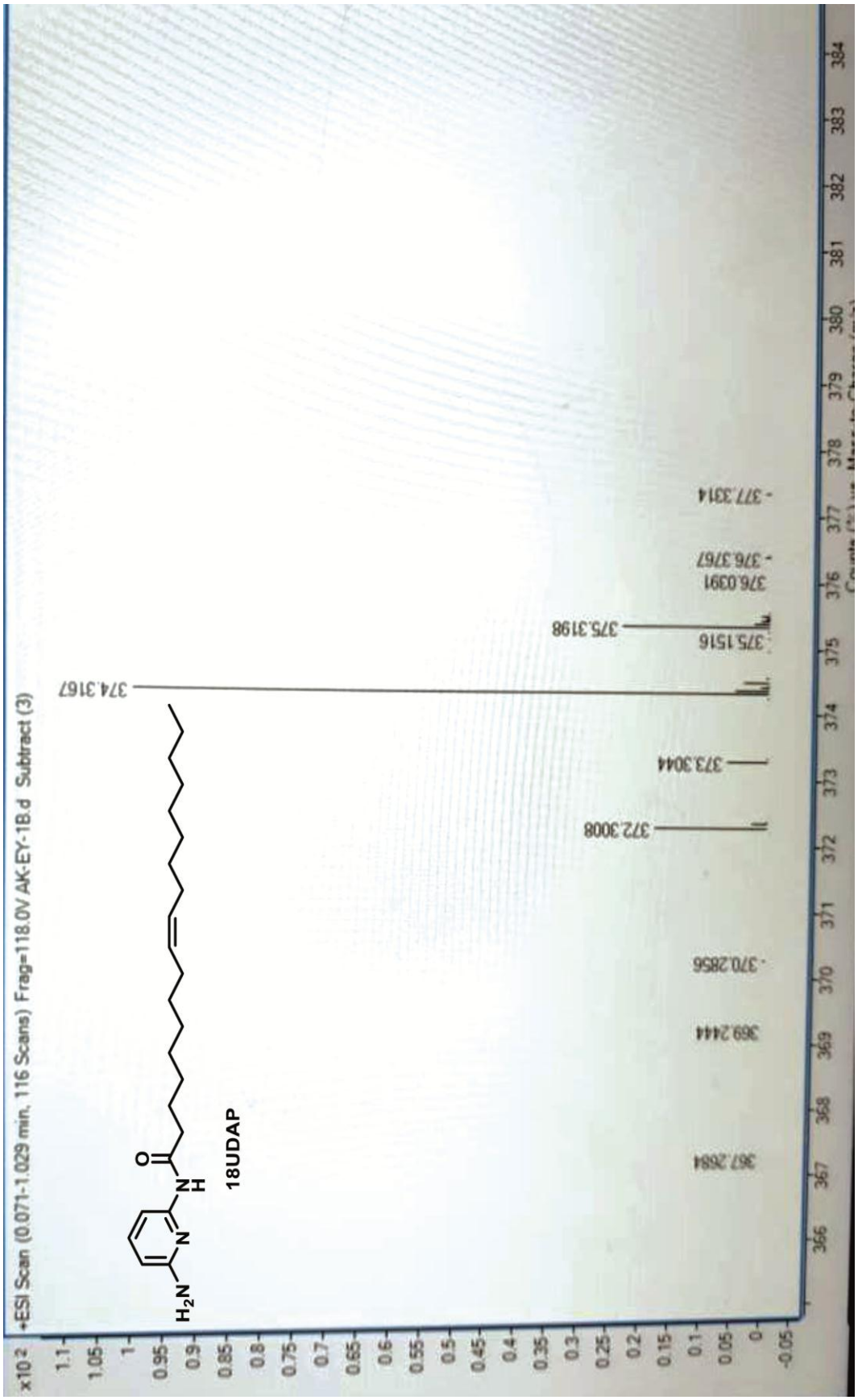

Figure 2.24. High resolution mass spectrum (HRMS) of **18UDAP**

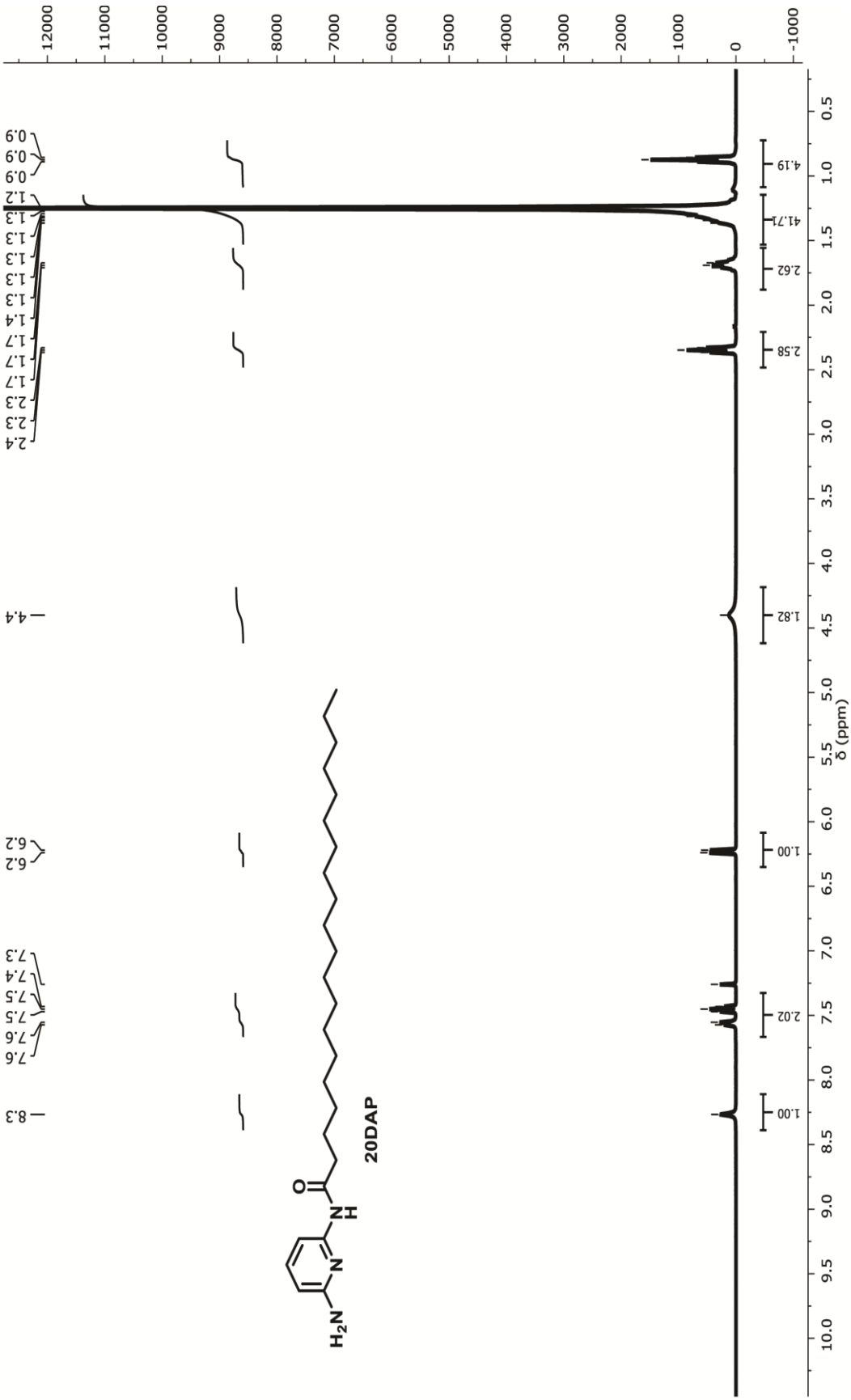

Figure 2.25. ^{1}H NMR spectrum of **20DAP** in $CDCl_3$ (400 MHz)

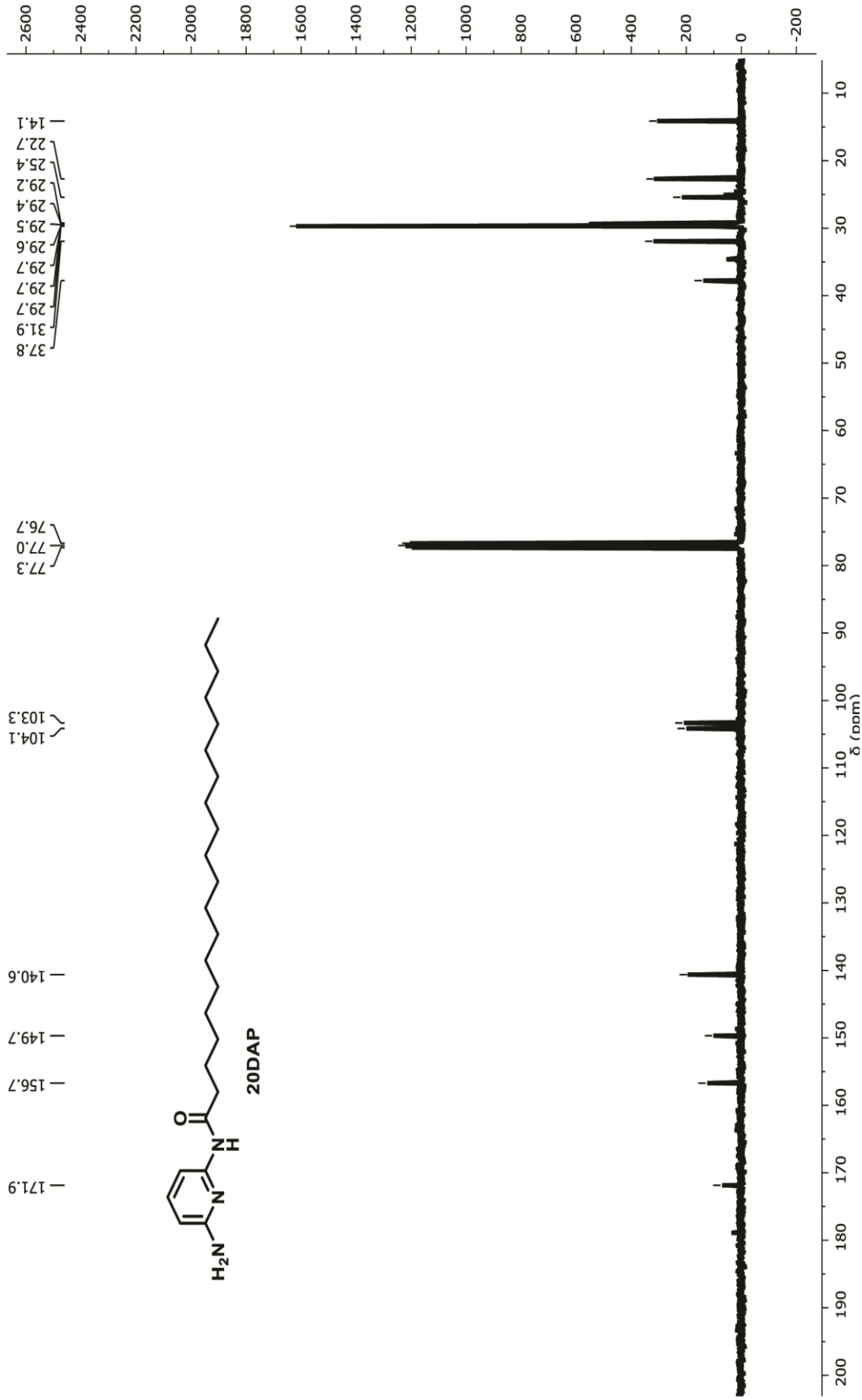

Figure 2.26. ^{13}C NMR spectrum of **20DAP** in $CDCl_3$ (100 MHz)

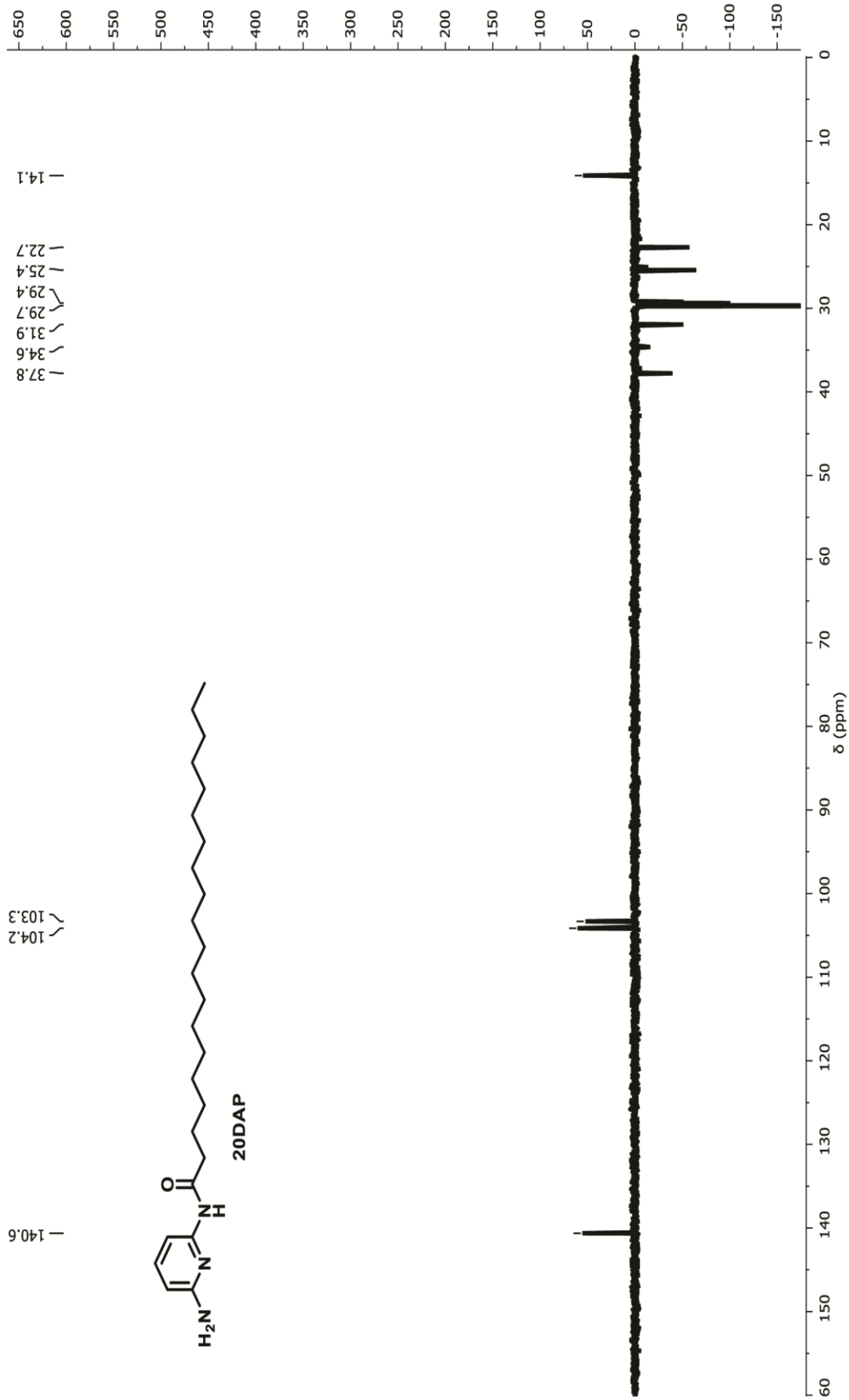

Figure 2.27. ^{13}C NMR (Dept-135) spectrum of **20DAP** in $CDCl_3$ (100 MHz)

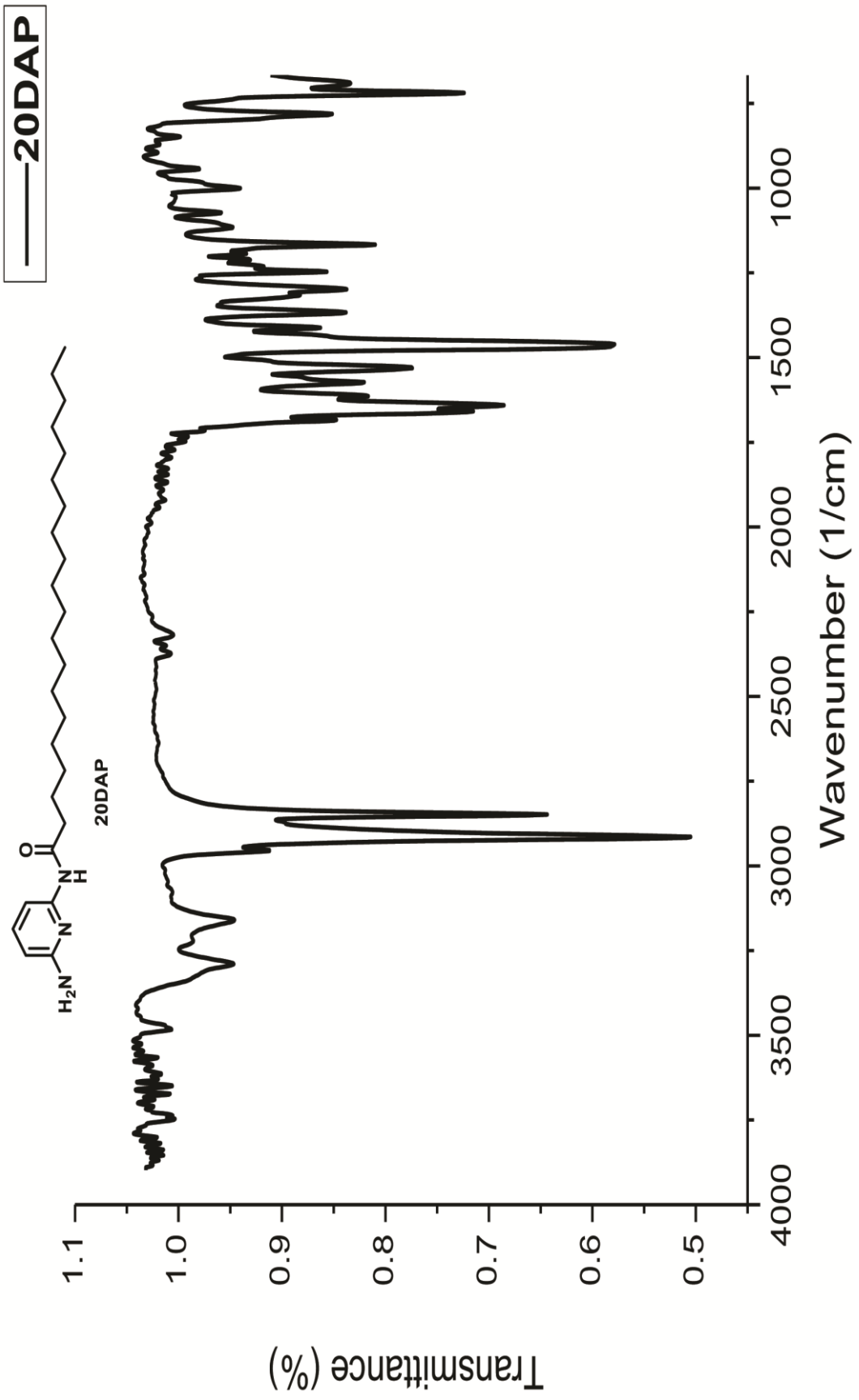

Figure 2.28. IR spectrum of **20DAP**

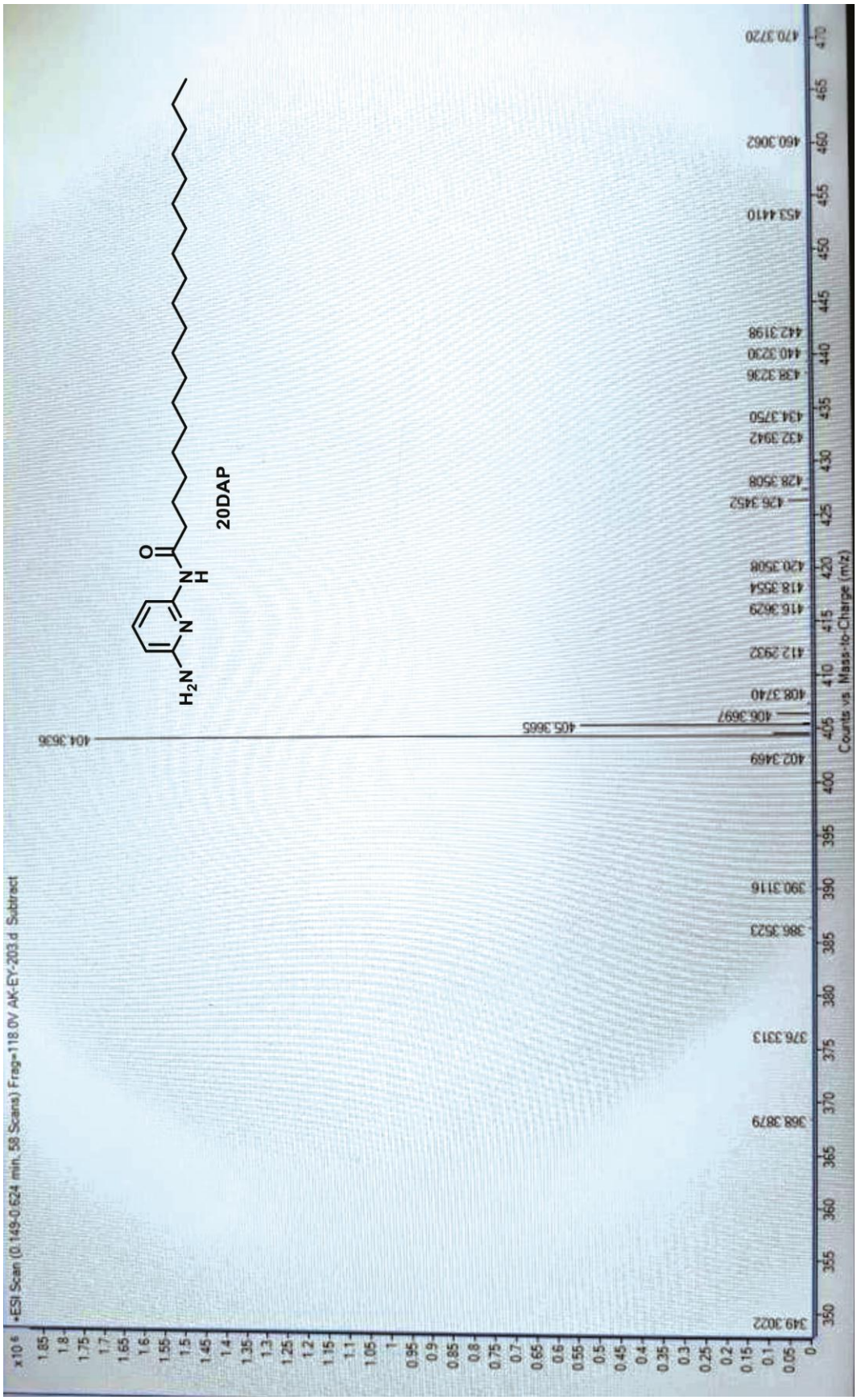

Figure 2.29. High resolution mass spectrum (HRMS) of **20DAP**

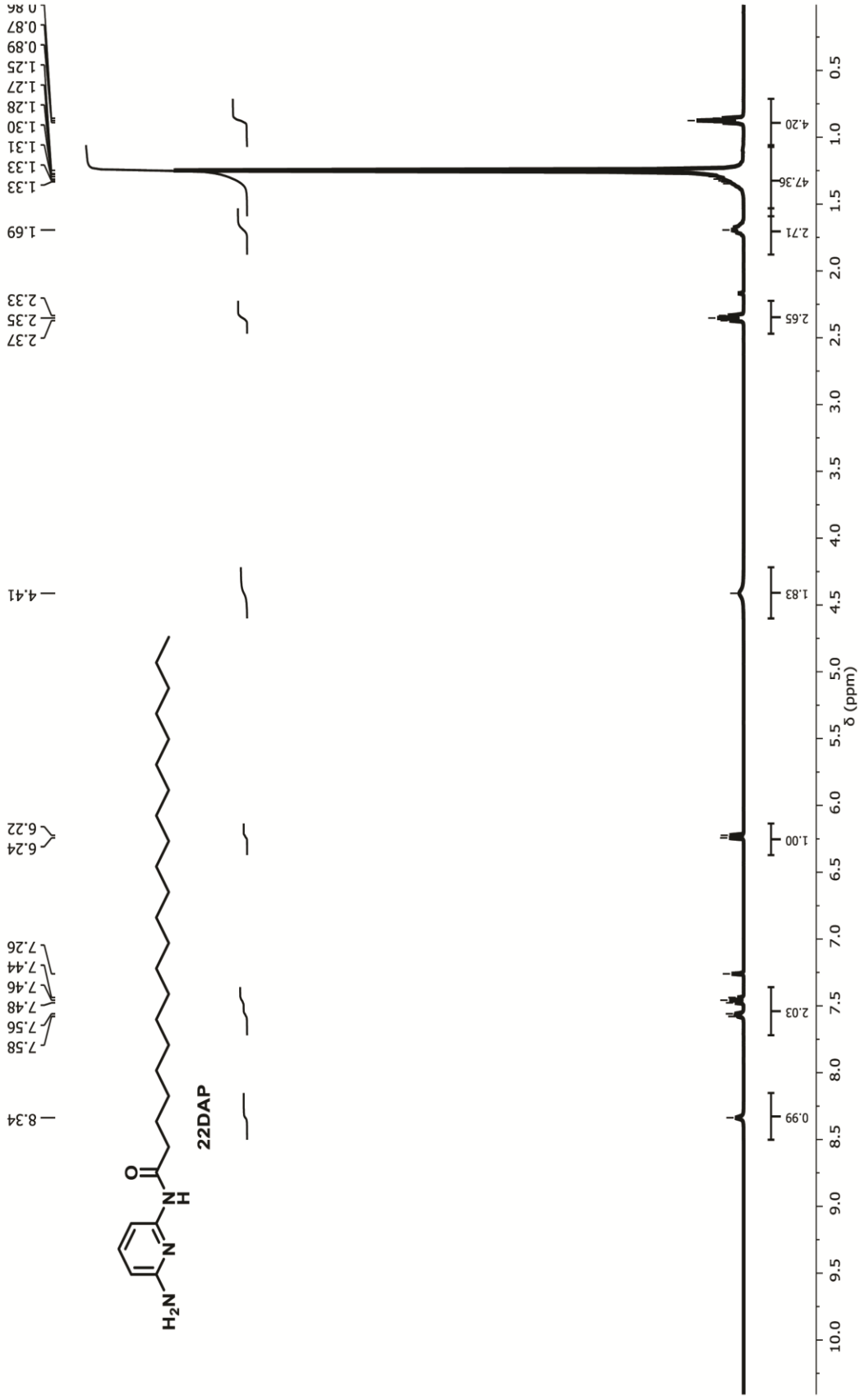

Figure 2.30. ^{1}H NMR spectrum of **22DAP** in $CDCl_3$ (400 MHz)

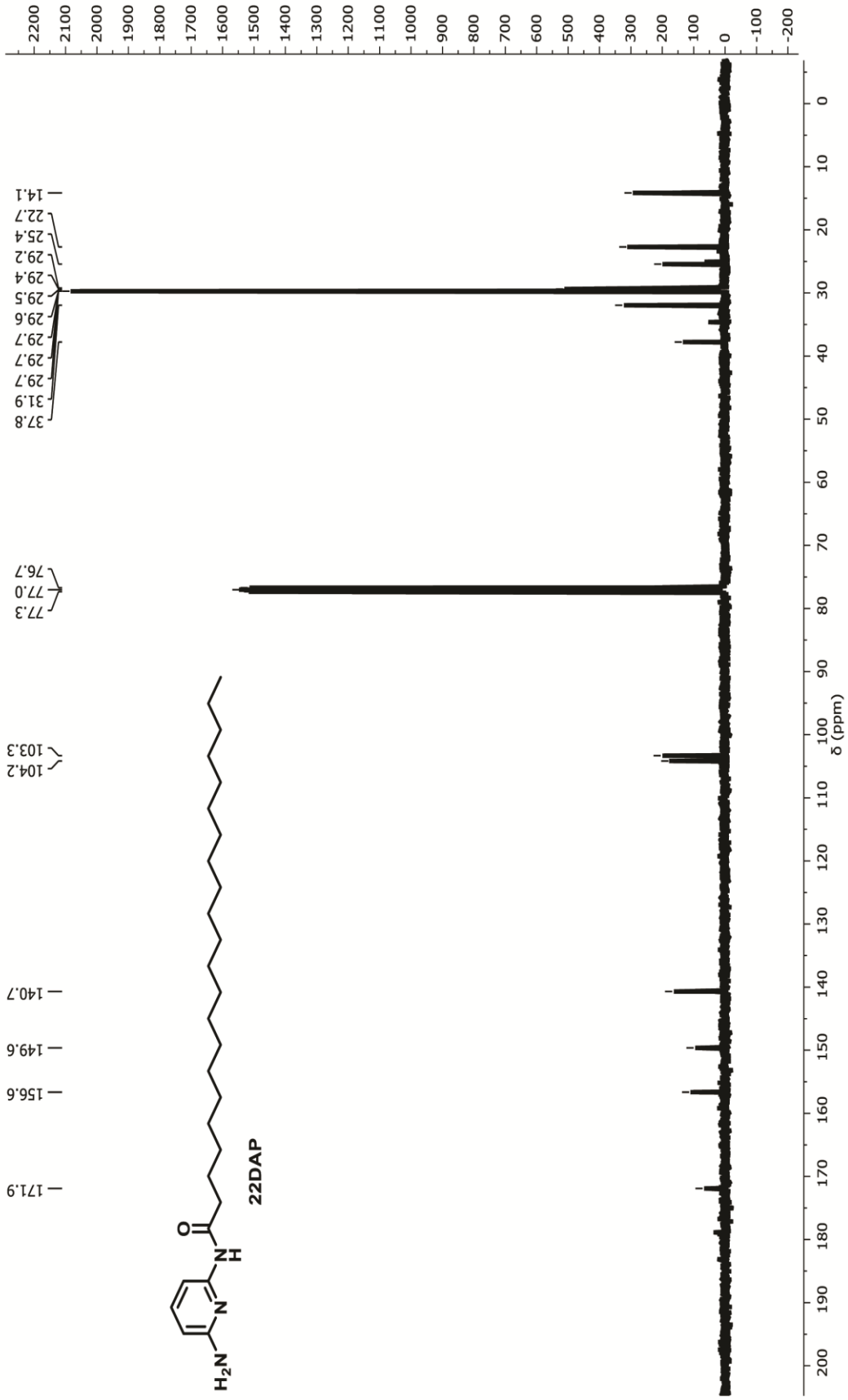

Figure 2.31. ^{13}C NMR spectrum of **22DAP** in $CDCl_3$ (100 MHz)

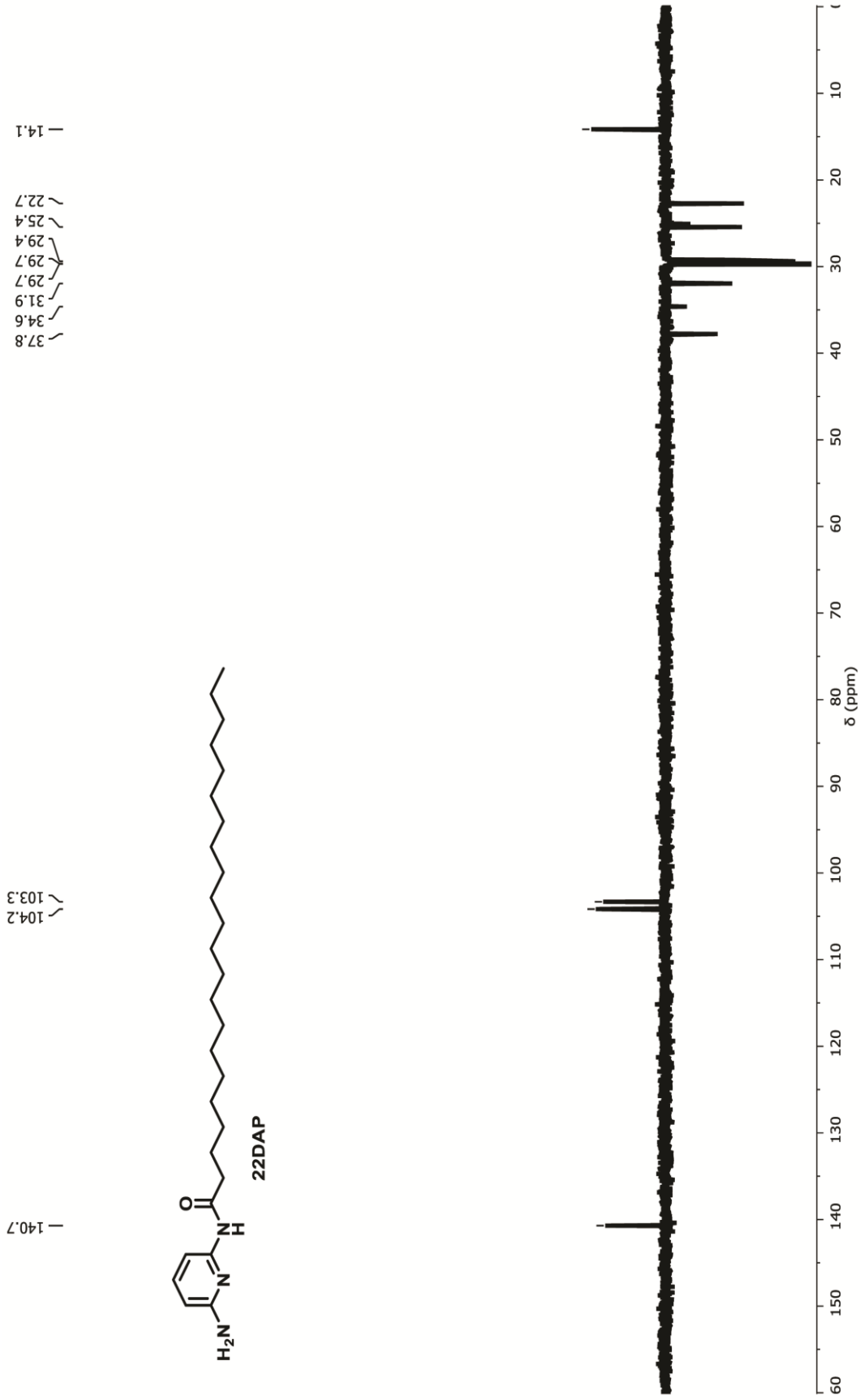

Figure 2.32. ^{13}C NMR (Dept-135) spectrum of **22DAP** in $CDCl_3$ (100 MHz)

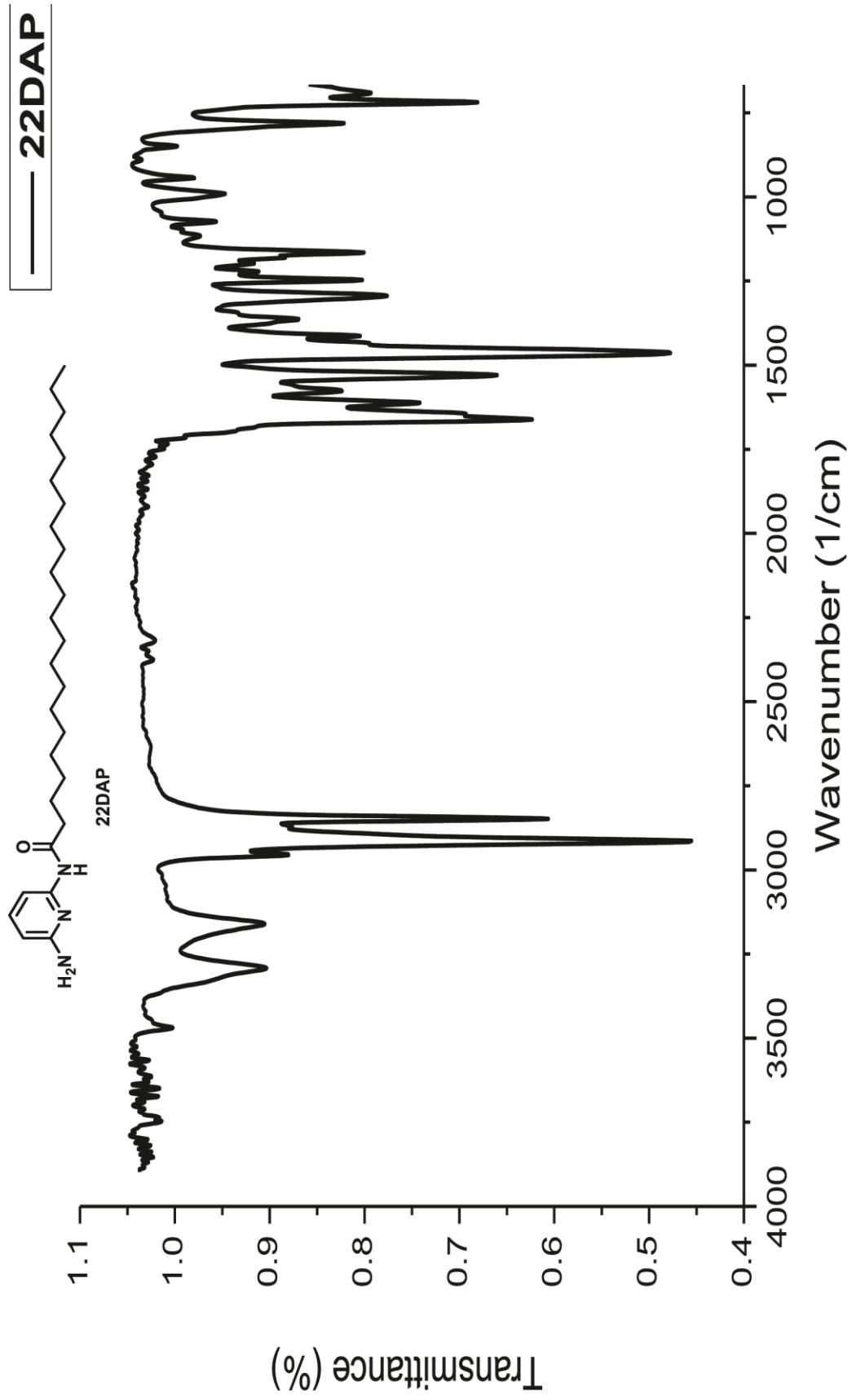

Figure 2.33. IR spectrum of **22DAP**

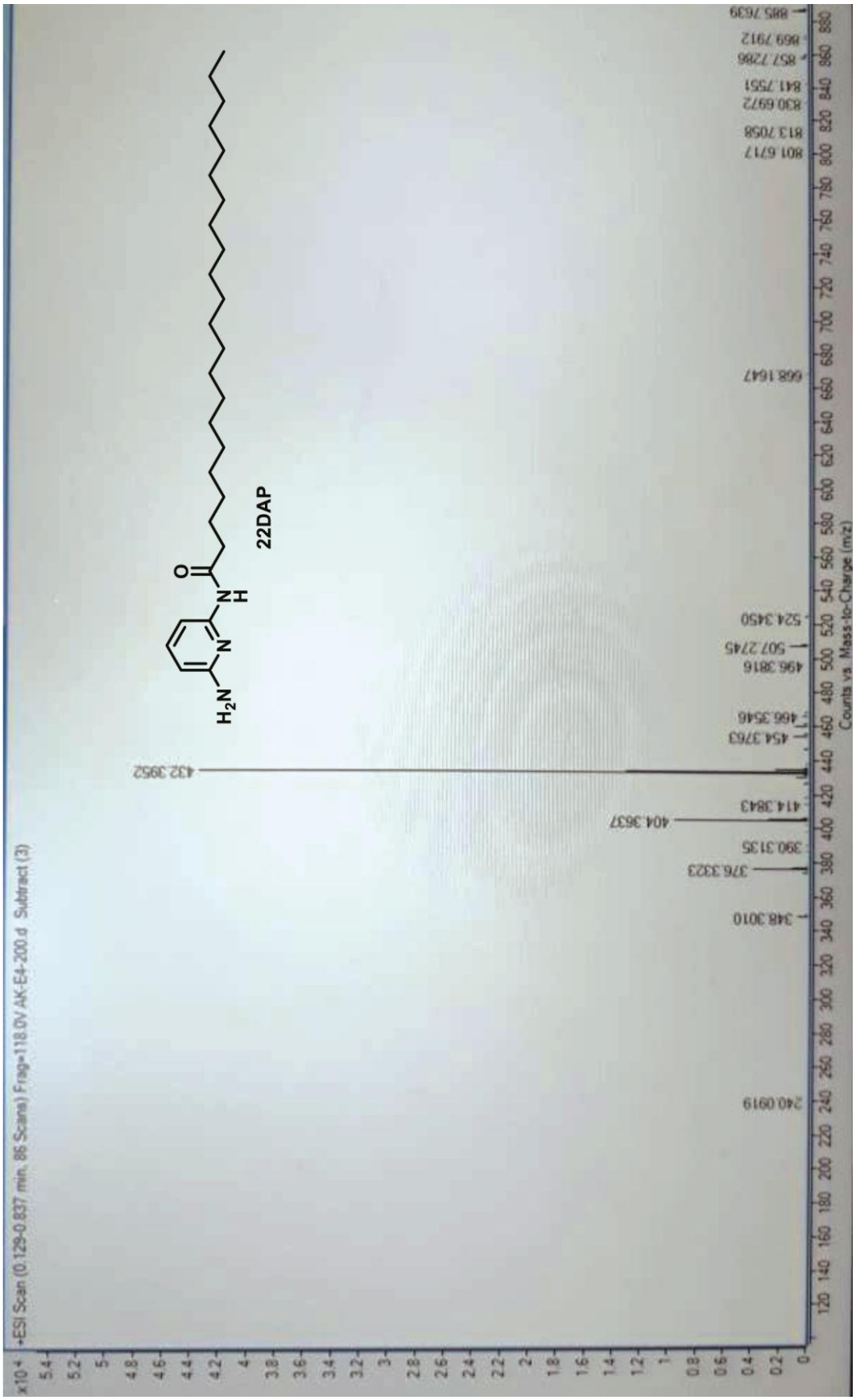

Figure 2.34. High resolution mass spectrum (HRMS) of **22DAP**

2.15 References

1. *(a)* S. Song, B. Tian, F. Chen, W. Zhang, Y. Pan, Q. Zhang, X. Yang and W. Pan, *Drug Dev. Ind. Pharm.*, 2015, **41**, 51-62; *(b)* M. Z. Ahmad, A. A. Mohammed and M. M. Ibrahim, *Pharm. Dev. Technol.*, 2016, **7450**, 1-10; *(c)* M. Z. Ahmad, S. Akhter, N. Mohsin, B. A. Abdel-Wahab, J. Ahmad, M. H. Warsi, M. Rahman, N. Mallick and F. J. Ahmad, *Curr. Drug Discovery Technol.*, 2014, **11**, 197-213.

2. V. B. Patravale, A. A. Date, R. M. Kulkarni, *J. Pharm. Pharmacol.*, 2004, **56**, 827.

3. *(a)* R. E. Kohman, S. S. Cha, H.-Y. Man and X. Han, *Nano Lett.*, 2016, **16**, 2781-2785; *(b)* S. Young, M. Wong, Y. Tabata and A. G. Mikos, *J. Control Release*, 2005, **109**, 256-274; *(c)* S. V. Bhosale and S. V. Bhosale, *Sci. Rep.*, 2013, **3**, 1982; *(d)* H. A. Strobel, E. I. Qendro, E. Alsberg and M. W. Rolle, *Front. Pharmacology*, 2018, **9**, 1229.

4. *(a)* E.-B. Lim, T. A. Vy and S.-W. Lee, *J. Mater. Chem. B*, 2020, **8**, 2096-2106; *(b)* B. A. Grzybowski, K. Fitzner, J. Paczesny and S. Granick, *Chem. Soc. Rev.*, 2017, **46**, 5647-5678; *(c)* C. M. Dias, H. Li, H. Valkenier, L. E. Karagiannidis, P. A. Gale, D. N. Sheppard and A. P. Davis, *Org. Biomol. Chem.* 2018, **16**, 1083-1087. W. Cui, J. Li and G. Decher, *Adv. Mater.*, 2016, **28**, 1302-1311; *(d)* A. Fuertes, M. Juanes, J. R. Granja and J. Montenegro, *Chem. Commun.*, 2017, **53**, 7861-7871; *(e)* F. Din, W. Aman, I. Ullah, O. S. Qureshi, O. Mustapha, S. Shafique and A. Zeb, *Int. J. Nanomedicine*, 2017, **12**, 7291-7309. *(f)* N. Machinaga, G. W. Ashley, R. Reid, A. Yamasaki, K. Tanaka, K. Nakamura, Y. Yabe, Y. Yoshigae and D. V. Santi, *TVST*, 2018, **7**, 21; *(g)* H. Li, H. Valkenier, A. G. Thorne, C. M. Dias, J. A. Cooper, M. Kieffer, N. Busschaert, P. A. Gale, D. N. Sheppard and A. P. Davis, *Chem. Sci.*, 2019, **10**, 9663-9672.

5. *(a)* J. Mayr, C. Saldías and D. D. Díaz, *Chem. Soc. Rev.*, 2018, **47**, 1484-1515; *(b)* S. Lange, J. Unsleber, P. Drücker, H. Galla, M. P. Waller and B. J. Ravoo, *Org. Biomol. Chem.*, 2015, **13**, 561-569; *(c)* L. Liu, W. D. Yao, Y. F. Rao, X. Y.

Lu and J. Q. Gao, *Drug Delivery*, 2017, **24**, 569-581; *(d)* S. Roy, M. Maiti, S. Das and A. Roy, *Chem. Papers*, 2020, **74**, 183-196; *(e)* K. P. C. Sekhar, D. K. Swain, S. A. Holey, S. Bojja and R. R. Nayak, *Langmuir*, 2020, **36**, 3080-3088. *(f)* K. P. C. Sekhar, H. Adicherla and R. R. Nayak, *Langmuir*, 2018, **34**, 8875-8886.

6. E. D. Co and A. G. Marangoni, *J. Am. Oil Chem. Soc.*, 2012, **89**, 749-780.

7. K. Rehman and M. H. Zulfakar, *Drug Dev. Ind. Pharm.*, 2014, **40**, 433-440.

8. *(a)* P. McNeice, Y. Zhao, J. Wang, G. F. Donnelly and P. C. Marr, *Green Chem.*, 2017, **19**, 4690-4697; *(b)* C. S. Hawes, A. D. Lynes, K. Byrne, W. Schmitt, G. Ryan, M. E. Mobius and T. Gunnlaugsson, *Chem. Commun*., 2017, **53**, 5989-5992; *(c)* Z. Li, Y. Huang, D. Fan, H. Li, S. Liu and L. Wang, *Front. Chem. Sci. Eng.*, 2016, **10**, 552-561; *(d)* D. Kong, Y. Xia, D. Li and R. Hou, *Supramol. Chem.*, 2017, **29**, 102-110; *(e)* C.-W. Chu and B. J. Ravoo, *Chem. Commun.*, 2017, **53**, 12450-12453; *(f)* Y. G. Jia, J. Jin, S. Liu, L. Ren, J. Luo and X. X. Zhu, *Biomacromolecules*, 2018, **19**, 626-632.

9. *(a)* C. Tsitsilianis, G. Serras, C.-H. Ko, F. Jung, C. M. Papadakis, M. Rikkou-Kalourkoti, C. S. Patrickios, R. Schweins and C. Chassenieux, *Macromolecules*, 2018, **51**, 2169-2179; *(b)* Y. Zhang, J. Ji, H. Li, N. Du, S. Song and W. Hou, *Soft Matter*., 2018, **51**, 2169-2179; *(c)* Z. Li, H. Bai, S. Zhang, W. Wang, P. Ma and W. Dong, *New J. Chem.*, 2018, **42**, 13453-13460.

10. *(a)* R. G. Weiss, *J. Am. Chem. Soc.*, 2014, **136**, 7519-7530; *(b)* K. J. Skilling, F. Citossi, T. D. Bradshaw, M. Ashford, B. Kellam and M. Marlow, *Soft Matter*, 2014, **10**, 237-256.

11. N. A. Peppas, P. Bures, W. Leobandung and H. Ichikawa, *Eur. J. Pharm. Biopharm.*, 2000, **50**, 27-46.

12. *(a)* P. Terech and R. G. Weiss, *Chem. Rev.*, 1997, **97**, 3133-3159; *(b)* W. L. Hinze, I. Uemasu, F. Dai and J. M. Braun, *Curr. Opin. Colloid Interface Sci.*, 1996, **1**, 502-513.

13. *(a)* S. Murdan, B. Ven den Bergh, G. Gregoriadis and A. T. Florence, *J. Pharm. Sci.*, 1999, **88**, 615-619; *(b)* J. H. Van Esch and B. L. Feringa, *Angew Chem. Int. Ed. Engl.*, 2000, **39**, 2263-2266; *(c)* H. Willimann, P. Walde, P. L. Luisi, A. Gazzaniga and F. Stroppolo, *J. Pharm. Sci.*, 1992, **81**, 871-874.

14. Z. Wei, J. H. Yang, J. Zhou, F. Xu, M. Zrinyi, P. H. Dussault, Y. Osada and Y. M. Chen, *Chem. Soc. Rev.*, 2014, **43**, 8114-8131.

15. *(a)* A. R. Patel, P. S. Rajarethinem, A. Gredowska, O. Turhan, A. Lesaffer, W. H. De Vos, D. Van de Walle and K. Dewettinck, *Food Funct.*, 2014, **5**, 645-652; *(b)* A. R. Patel, N. Cludts, M. D. B. Sintang, A. Lesaffer and K. Dewettinck, *Food Funct.*, 2014, **5**, 2833-2841.

16. B. O. Okesola and D. K. Smith, *Chem. Soc. Rev.*, 2016, **45**, 4226-4251.

17. B. Behera, S. S. Sagiri, K. Pal and A. Srivastava, *J. Appl. Polym. Sci.*, 2013, **127**, 4910-4917.

18. W. L. Hinze, I. Uemasu, F. Dai and J. M. Braun, *Curr. Opin. Colloid Interface Sci.*, 1996, **1**, 502-513.

19. A. C. Couffin-Hoarau, A. Motulsky, P. Delmas, J. C. Leroux, *Pharm. Res.*, 2004, **21**, 454-457.

20. R. Langer, *Science*, 2001, **293**, 58-59.

21. M. C. Branco, D. J. Pochan, N. J. Wagner, J. P. Chneider, *Biomaterials*, 2009, **30,** 1339-1347.

22. S. Murdan, *Expert Opin. Drug Deliv*., 2005, **2**, 1-17.

23. T. P. Sangale, V. G. Gadhave Manoj, *World J. Pharm. Res.*, 2015, **4**, 423-442.

24. K. Hanabusa, M. Matsumoto, M. Kimura, A. Kakehi, H. J. Shirai, *Colloid Interface Sci.*, 2000, **224**, 231-244.

25. S. Gupta, R. P. Singh, A. Sarkar, H. Panchai, D. Pandey, *Pharm. Glob. (IJCP),* 2011, **5**.

26. G. Tarun, B. Ajay, K. Bhawana, K. Sunil, Ravi, *Int. J. Res. Pharm.*, 2011, **2**, 15-21.

27. A. Blumlein and J. J. McManus, *J. Mater. Chem. B*, 2015, **3**, 3429-3435.

28. V. K. Singh, I. Banerjee, T. Agarwal, K. Pramanik, M. K. Bhattacharya and K. Pal, *Colloids Surf. B: Biointerfaces.,* 2014, **123**, 582-592.

29. I. Almeida, A. Fernandes, L. Fernandes, M. Pena Ferreira, P. Costa, M. Bahia, *Pharm. Dev. Technol.,* 2008, **13**, 487–494.

30. K. Rehman, M.H. Zulfakar, *Drug Dev. Ind. Pharm*., 2013, **40**, 433–440.

31. F. Varrato, L. Di Michele, M. Belushkin, N. Dorsaz, S.H. Nathan, E. Eiser, G. Foffi, *Proc. Natl. Acad. Sci*., 2012, **109**, 19155–19160.

32. L. Di Michele, F. Varrato, D. Fiocco, S. Sastry, E. Eiser, G. Foffi, *Soft Matter*, 2014, **10**, 3633–3648.

33. M. M. Ibrahim, S. A. Hafez, M. M. Mahdy, *Asian J. Pharm. Sci*., 2013, **8**, 48-57.

34. B. Behera, S. S. Sagiri, K. Pal, K. Pramanik, U. A. Rana, I. Shakir and A. Anis, *Polym. Plast. Technol. Eng.*, 2015, **54**, 837-850.

35. B. Behera, S. S. Sagiri, V. K. Singh, K. Pal and A. Anis, *Starch-Starke*., 2014, **66**, 865-879.

36. I. Almeida, A. Fernandes, L. Fernandes, M. Pena Ferreira, P. Costa and M. Bahia, *Pharm. Dev. Technol.,* 2008, **13**, 487-494.

37. L. Di Michele, D. Fiocco, F. Varrato, S. Sastry, E. Eiser and G. Foffi, *Soft Matter,* 2014, **10**, 3633-3648.

38. M. N. Lee and A. Mohraz, *Adv. Matter*, 2010, **22**, 4836-4841.

39. V. K. Singh, A. Anis, S. Al-Zahrani, D. K. Pradhan and K. Pal, *Int. J. Electrochem. Sci.*, 2014, **9**, 5049-5060.

40. S. Gupta, R. P. Singh, A. Sarkar, H. Panchai, D. Pandey, *Pharm. Glob. (IJCP),* 2011, 5.

41. G. Tarun, B. Ajay, K. Bhawna, K. Sunil, J. Ravi, *Int. Res. Pharm.*, 2011, **2**, 15-21.

42. B. Hu, W. Wang, Y. Wang, *Mater Sci Eng C Mater Biol Appl.*, 2018, **82**, 80–90.

43. Z. Li, J. Cao, B. Hu, *Drug Dev. Ind. Pharm.*, 2016, **42**, 1732–1741.

44. Z. Li, J. Cao, H. Li, *Drug Deliv.*, 2016, **23**, 3168–3178.

45. B. Hu, W. Sun, H. Li, *Int. J. Pharm.*, 2018, **547**,637–647.

46. B. Hu, H. Yan, Yanping Sun, X. Chen, Yujuan Sun, S. Li, Y. Jing, H. Li, *Aertificiall Cells, Nanomedicine and Biotechnology*, 2020, **48**, 266-275.

47. A. Pal, Y. K. Ghosh, S. Bhattacharya, *Tetrahedron*, 2007, **63**, 7334-7348.

48. *(a)* S. Chang, A. D. Hamilton, *J. Am. Chem. Soc*., 1988, **110**, 1318; *(b)* S. Chang, D. Van Engen, E. Fan, A. D. Hamilton, *J. Am. Chem. Soc.*, 1991, **113**, 7640.

49. M. Mazik, D. Blaser, R. Boese, *Tetrahedron*, 1999, **55**, 12771.

50. *(a)* J. S. Yadav, M. K. Gupta, I. Prathap, M. P. Bhadra, P. K. Mohan and B. Jagannadh, *Chem. Commun.*, 2007, **37**, 3832-3834; *(b)* J. S. Yadav and M. K. Gupta, *Int. J. Phar. Sci. Res.*, 2012, **3**, 4822-4826.

51. M. F. Hassan, A. Rauf, *J. Nanostruct. Chem.*, 2014, **4**, 83-93.

52. B. A. Kumar and R. R. Nayak, *New J. Chem.*, 2019, **43**, 5559-5567.

53. K. J. C. van Bommel, M. C. Stuart, B. L. Feringa and J. van Esch, *Org. Biomol. Chem.*, 2005, **3**, 2917-2920.

54. G. John, M. Mason, P. M. Ajayan and J. S. Dordick, *J. Am. Chem. Soc.*, 2004, **126**, 15012-15013.

55. F. H. Beijer, R. P. Sijbesma, J. A. J. M. Vekemans, E. W. Meijer, H. Koojman and A. Spek, *J. Org. Chem.*, 1996, **61**, 6371-6380.

56. *(a)* K. Lalitha, Y. S. Prasad, C. U. Maheswari, V. Sridharan, G. John and S. Nagarajan, *J. Mater. Chem. B*, 2015, **3**, 5560-5568; *(b)* J. Liu, C. Detrembleur, A. Debuigne, M. C. De Pauw-Gillet, S. Mornet, L. Vander Elst, S. Laurant, E. Duguet and C. Jerome, *J. Mater. Chem. B*, 2014, **2**, 1009-1023.